P4-ATPase endosomal recycling relies on multiple retromer-dependent localization signals

Mariana Jiménez, Claire K. Kyoung, Kateryna Nabukhotna, Davia Watkins, Bhawik K. Jain, Jordan T. Best, and Todd R. Graham*
Department of Biological Sciences, Vanderbilt University, Nashville, TN 37235

ABSTRACT **Type IV P-type ATPases (P4-ATPases) are lipid flippases that generate an asymmetric membrane organization essential for cell viability. The five budding yeast P4-ATPases traffic between the Golgi complex, plasma membrane, and endosomes but how they are recycled from the endolysosomal system to the Golgi complex is poorly understood. In this study, we find that P4-ATPase endosomal recycling is primarily driven by the retromer complex and the F-box protein Rcy1. Defects in P4-ATPase recycling result in their mislocalization to the vacuole and a substantial loss of membrane asymmetry. The P4-ATPases contain multiple predicted retromer sorting signals, and the characterization of these signals in Dnf1 and Dnf2 led to the identification of a novel retromer-dependent signal, IPM[ST] that acts redundantly with predicted motifs. Together, these results emphasize the importance of endosomal recycling for the functional localization of P4-ATPases and membrane organization.**

SIGNIFICANCE STATEMENT

- P4-ATPase intracellular trafficking is critical for establishing cell membrane asymmetry; however, their recycling from the endolysosomal system to the Golgi is complex and poorly understood.
- Using *Saccharomyces cerevisiae*, the authors found that the retromer complex is the primary driver of P4-ATPase recycling out of the endolysosomal system and further characterized a novel retromer-dependent sorting signal, IPM[TS]. In addition, P4-ATPase mislocalization in retromer mutants causes significant changes in membrane organization.
- As both P4-ATPase and retromer deficiency are linked to human neurological disease, their role in membrane organization may be a key factor in neurodegeneration.

Monitoring Editor
Mary Munson
University of Massachusetts Medical School

Received: May 13, 2024
Revised: Jul 15, 2024
Accepted: Jul 30, 2024

This article was published online ahead of print in MBoC in Press (http://www.molbiolcell.org/cgi/doi/10.1091/mbc.E24-05-0209) on Aug 7, 2024.

Author contributions: M.J. and T.R.G. conceived and designed the experiments; M.J. and K.N. performed the experiments; M.J., C.K.K., K.N., and D.W. analyzed the data; M.J. and T.R.G. drafted the article; M.J. prepared the digital images; B.K.J. methodology: reviewed and edited writing; J.B. methodology: review and edit writing.

Conflicts of interest: The authors declare no financial conflict of interest.

*Address Correspondence to: Todd R. Graham (tr.graham@vanderbilt.edu).

Abbreviations used: CT, carboxy-terminal tail; NT, amino-terminal tail; PC, phosphatidylcholine; PE, phosphatidylethanolamine; PM, plasma membrane; PS, phosphatidylserine; P4-ATPase, type IV P-type ATPase.

INTRODUCTION

The function of each membrane-bound organelle in eukaryotic cells is determined by their unique protein and lipid composition. Most of the protein and lipid content for organelles within the secretory and endocytic pathways is initially synthesized at the endoplasmic reticulum (ER), and newly synthesized membrane proteins rely on vesicular transport mechanisms for delivery to their final destinations (Bonifacino and Glick, 2004; Burd and Cullen, 2014). During lipid synthesis, the rapid and energy-independent flip-flop of lipids in the ER membrane allows for the balanced growth of both leaflets (Bishop and Bell, 1988). The lipids can then be delivered by both vesicular and nonvesicular transport mechanisms to all other cellular membranes. A critical aspect of both membrane biogenesis and protein trafficking in the endomembrane system is the generation of membrane asymmetry between the two leaflets of the Golgi and plasma membrane, which is driven by the lipid flippases in the type IV P-type ATPase (P4-ATPase) family (Sebastian *et al.*, 2012; Roland and Graham, 2016; Best *et al.*, 2019).

The P4-ATPases harness ATP hydrolysis to transport lipid substrates from the exofacial to the cytofacial leaflet of the membrane against the prevailing concentration gradient. There are five members of the P4-ATPase family in *Saccharomyces cerevisiae*, Neo1, Drs2, Dnf1, Dnf2, and Dnf3, each with its own lipid substrate specificity and subcellular localization. With the exception of Neo1, the P4-ATPases form a functional complex with a respective β-subunit, necessary for exit out of the ER (Saito *et al.*, 2004). Drs2, Neo1, and Dnf3 are primarily localized to the Golgi complex while a significant fraction of Dnf1 and Dnf2 localize to the plasma membrane (Hua *et al.*, 2002; Hua and Graham, 2003; Natarajan *et al.*, 2004). The Golgi P4-ATPases all appear to transport phosphatidylserine (PS) and phosphatidylethanolamine (PE) to concentrate these phospholipids in the cytosolic leaflet, and this asymmetric organization is maintained as the membrane moves from the Golgi to the plasma membrane (Natarajan *et al.*, 2004; Alder-Baerens *et al.*, 2006; Zhou and Graham, 2009; Frøsig *et al.*, 2020). Dnf1 and Dnf2 transport PE and phosphatidylcholine (PC) such that the combined action of all of the P4-ATPases results in plasma membrane asymmetry characterized by enrichment of PS, PE, and PC in the cytosolic leaflet and glycosphingolipids in the extracellular leaflet (Kato *et al.*, 2002; Pomorski *et al.*, 2003; Iyoshi *et al.*, 2014; Roland *et al.*, 2019). At varying points in time, all these flippases pass through the endosomal system as part of their trafficking itinerary; therefore, they must be recycled out of endosomes back to their primary site of localization. Except for Neo1 (Wu *et al.*, 2016; Dalton *et al.*, 2017), the pathways and sorting signals used to recycle P4-ATPases have not been characterized.

Recycling out of the endosomal system is highly dynamic, and many coated carriers are involved in removing cargo from endosome-lysosomal organelles and directing them back to the Golgi (Burd and Cullen, 2014; Best *et al.*, 2020; Suzuki *et al.*, 2021). In budding yeast, the recycling pathways for endosome-to-Golgi trafficking of most cargoes are mediated by one or more of Rcy1, Snx4, and Retromer (Figure 1A). Retromer is composed of a trimeric cargo recognition complex formed by the Vps26, Vps29, and Vps35 subunits, which associates with the auxiliary, membrane interacting sorting nexins, Vps5-Vps17 heterodimers, or Snx3 homodimers. Retromer also forms a complex with Atg18, which is important for vacuolar fragmentation induced by hyperosmotic stress (Krick *et al.*, 2008; Courtellemont *et al.*, 2022; Marquardt *et al.*, 2023). Retromer can identify a range of cargo through its interaction with several cargo sorting motifs; notable ones include Ω-ϕ-L/M/V, Ω-x-x-L/M/V, Ω-E-(F/L), or FxFxD consensus sequences (Ω, aromatic; ϕ, hydrophobic) (Cooper and Stevens, 1996; Voos and Stevens, 1998; Finnigan *et al.*, 2012; Fjorback *et al.*, 2012; Bean *et al.*, 2017; Suzuki *et al.*, 2019). The first retromer cargo discovered was Vps10 in budding yeast and over 150 cargos are currently known to depend on retromer sorting within the mammalian endosomal system (Seaman *et al.*, 1997; Burd and Cullen, 2014). Neo1 contains a FEM motif (a variant of Ω-E-(F/L)) and is a known Snx3-retromer cargo (Wu *et al.*, 2016; Dalton *et al.*, 2017). The second endosomal recycling pathway in yeast is mediated by two distinct heterodimers containing Snx4, Snx4-Atg20, and Snx4-Snx42, that function to recycle cargos such as Snc1 and Atg27 out of the endosomes back to the Golgi and can also help initiate the autophagic cytoplasm-to-vacuole targeting pathway (Dalton *et al.*, 2017; Ma *et al.*, 2018). These Snx4 heterodimers have been shown to function redundantly with retromer for multiple cargoes, including the Atg9 scramblase (Hettema *et al.*, 2003; Ravussin *et al.*, 2021). Furthermore, Snx4 may play a role in removing cargo from the vacuole membrane for delivery to endosomes, where retromer can then mediate delivery to the Golgi (Suzuki and Emr, 2018). Another recycling pathway of interest is mediated by Rcy1, an F-box protein that facilitates the ubiquitin and COPI-dependent recycling of a v-SNARE, Snc1, from the endosomal system back to the Golgi (Chen *et al.*, 2005; Furuta *et al.*, 2007; Hanamatsu *et al.*, 2014; Xu *et al.*, 2017; Date *et al.*, 2022). In addition to Snc1, the pheromone receptors Ste2 and Ste3, and nutrient transporters Mup1 and Tat2 are among the few cargoes known to require Rcy1 for their localization (Lewis *et al.*, 2000; Wiederkehr *et al.*, 2000; MacDonald and Piper, 2017). The Rcy1, Snx4, and retromer pathways all appear to function independently and in parallel to each other for endosome → Golgi transport (Best *et al.*, 2020).

Translocation of lipid substrates by P4-ATPases induces bending of the membrane into the cytosol, which can facilitate vesicle budding for trafficking pathways departing the Golgi and/or endosomal compartments. Neo1 is required for COPI-dependent Golgi to ER transport and the ability of Snx3-retromer to sort other cargoes from endosomes (Hua and Graham, 2003; Dalton *et al.*, 2017). Similarly, the metazoan orthologue of Neo1, ATP9A, is required for SNX3-retromer function in recycling Wntless, and therefore impacts Wnt signaling (McGough *et al.*, 2018). Drs2 and the Dnf1 P4-ATPases act redundantly to facilitate protein sorting by AP-3 or GGA/clathrin, and loss of Drs2 alone is sufficient to disrupt AP-1/clathrin function in yeast cells (Hua *et al.*, 2002; Liu *et al.*, 2008). Along with initiating membrane curvature, PS translocation to the cytosolic leaflet can create a negatively charged microenvironment for effector recruitment (Xu *et al.*, 2013; Lee *et al.*, 2015; Matsudaira *et al.*, 2017). Furthermore, flippases not only act as a driver for transport but can be cargos for those same pathways; in the case of Drs2, loss of AP-1/clathrin increases the rate of Drs2 transport to the plasma membrane. Various groups have suggested that AP-1/clathrin carries cargo in both the anterograde and retrograde pathways between Golgi and endosomes, and potentially in intra-Golgi retrograde trafficking (Valdivia *et al.*, 2002; Ha *et al.*, 2003; Liu *et al.*, 2008; Casler *et al.*, 2022). Thus, the function of AP-1 in yeast remains somewhat enigmatic and its role in trafficking P4-ATPases other than Drs2 has not been defined.

Here we untangle the complexity of endosomal recycling pathways used to sort the P4-ATPases Neo1, Drs2, Dnf1, and Dnf2, all requiring retromer. We show that Rcy1 contributes to Drs2, Dnf1, and Dnf2 recycling, while Snx4 plays a minor role in Dnf1 recycling. We also discover a novel retromer-dependent sorting signal in Dnf1 and Dnf2, and the requirement for multiple

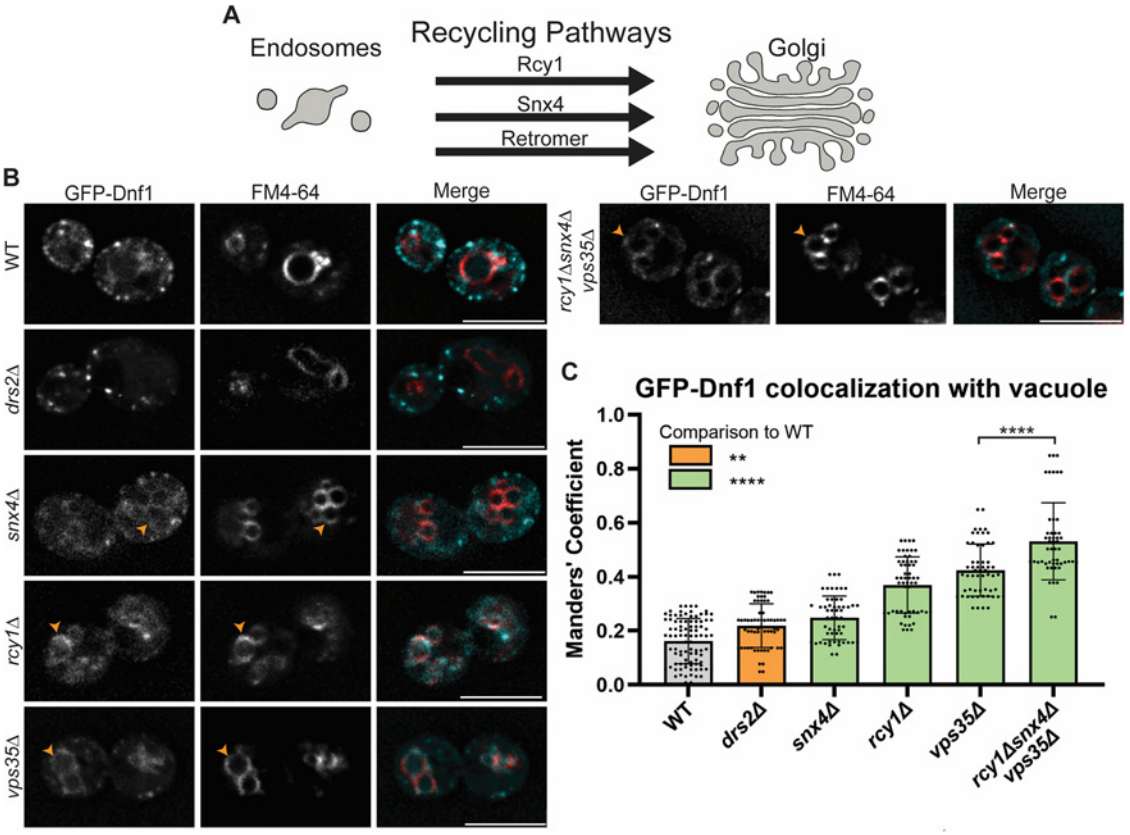

FIGURE 1: Dnf1 is primarily recycled by retromer while Rcy1 and Snx4 significantly contribute to its trafficking. (A) A model of yeast endosome to Golgi retrograde trafficking. (B) Localization of GFP-Dnf1 in retrograde mutants. Orange arrowheads point to GFP-Dnf1 localization at the vacuole limiting membrane. (C) Quantification via Manders' coefficient of the proportion of GFP-Dnf1 colocalized with FM4-64 (vacuole limiting membrane). For all quantification, data from ~60 cells from three independent experiments were obtained and analyzed. Comparisons calculated via a one-way ANOVA followed by a Tukey's post hoc test. Colors represent comparison to WT, pairwise comparisons shown with brackets and asterisk. $P < 0.01$ is ** (orange) and $P<0.0001$ is **** (green). Error bars represent SD. Scale bars: 5 AAm.

cargo sorting motifs to localize the flippases properly. Finally, we show that defects in P4-ATPase recycling led to their mislocalization to the vacuole and cause a loss of PE and PS membrane asymmetry.

RESULTS

P4-ATPases primarily use retromer for recycling

To test the routes used for P4-ATPase trafficking, we observed the localization of GFP or monomeric NeonGreen (mNG) tagged Dnf1, Dnf2, Drs2, and Neo1 in strains with deletions of major components of the Rcy1, Snx4, AP-1 and retromer pathways. In addition, we examined how *drs2*Δ influences trafficking of the other P4-ATPases as *drs2*Δ disrupts the trafficking of cargos sorted by AP-1 and Rcy1 (Hua *et al.*, 2002; Liu *et al.*, 2008). We found that loss of Rcy1 or Vps35, a major component of retromer, led to mislocalization of GFP-Dnf1 to the vacuole as seen by the circular ring marked by vacuolar dye FM4-64 (Figure 1, B and C). Meanwhile, the loss of Snx4 led to significant mislocalization of GFP-Dnf1 but to a lesser extent compared with loss of Rcy1 and Vps35. GFP-Dnf1 was slightly mislocalized to the vacuole of *drs2*Δ, while *apl4*Δ (AP-1 γ-subunit) had no effect on Dnf1 localization (Figure 1; Supplemental Figure S1). Combined loss of these three pathways in the *rcy1*Δ*snx4*Δ*vp35*Δ mutant caused the greatest extent of Dnf1 mislocalization to the vacuole (~60%), congruent with the notion that Dnf1 uses multiple different routes for recycling. Looking further into retromer's role in Dnf1 recycling, single mutations of SNX-BAR retromer components Vps5 and Vps17 yielded equivalent mislocalization to the vacuole as *vps35*Δ while loss of Snx3, another SNX-BAR protein, had a minor effect on Dnf1 localization (Supplemental Figure S1). Thus, Dnf1 appears to use retromer complexes with the Vps5-Vps17 heterodimers more frequently than retromer with Snx3 homodimers for recycling. Additionally, we quantified changes in Dnf1 localization with respect to the plasma membrane (PM) marker Ras2. We found that the large cell-to-cell variability in Dnf1 PM localization made this assay less sensitive for detecting Dnf1 trafficking defects than measuring colocalization with FM4-64 at the vacuole. Nonetheless, we found no loss in Dnf1 PM localization for *snx4*Δ, and the *rcy1*Δ strain displayed a small, but still significant decrease in PM localization. Consistently, strains harboring retromer mutations or retromer-Rcy1-Snx4 mutations showed the greatest loss of Dnf1 PM localization (Supplemental Figure S2). Together, these results indicate that Dnf1 is primarily recycled by retromer, but Rcy1 and Snx4 can significantly contribute to its trafficking.

For Dnf2-mNG, we found that *rcy1*Δ or *vps35*Δ deletions led to partial mislocalization to the vacuole but *snx4*Δ, *drs2*Δ, or *apl4*Δ deletions did not (Figure 2, A and B; Supplemental Figure S3). Loss of both Rcy1 and retromer in the *rcy1*Δ*vps35*Δ double mutant resulted in 45% mislocalization to the vacuole, which was

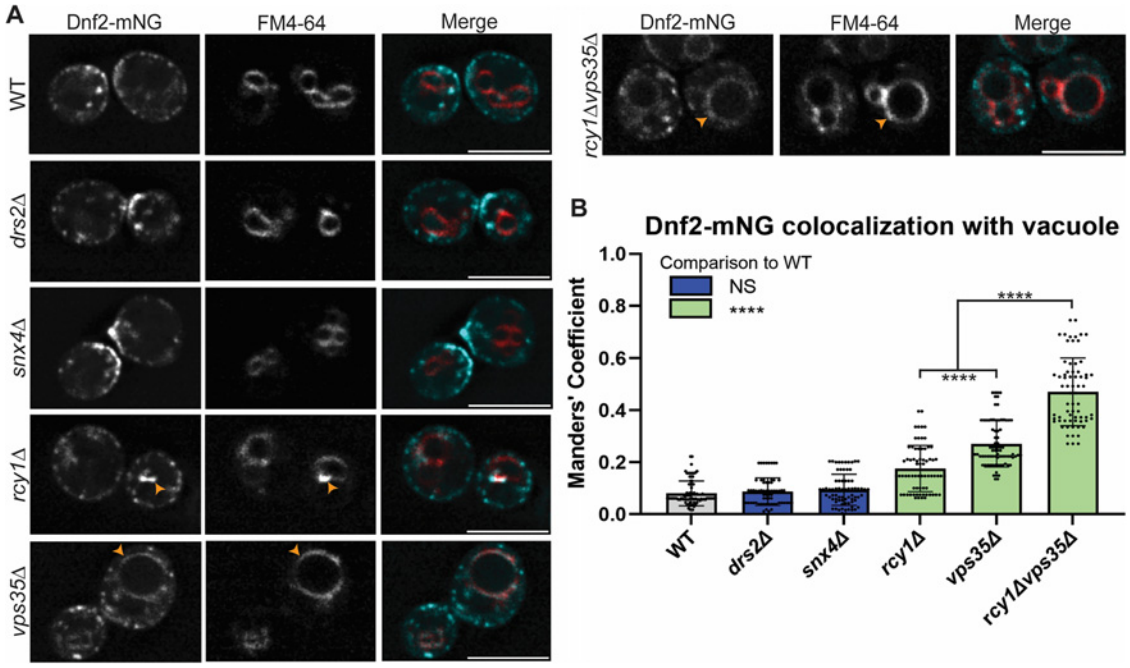

FIGURE 2: Retromer and Rcy1 contribute to Dnf2 recycling out of endosomes. (A) Localization of Dnf2-mNG in retrograde mutants. Orange arrowheads point to the localization of Dnf2-mNG to the vacuole limiting membrane. (B) Quantification via Manders' coefficient of the proportion of Dnf2-mNG colocalized with FM4-64 (vacuole limiting membrane). For all quantification, data from ~60 cells from three independent experiments were obtained and analyzed. Comparisons were calculated via a one-way ANOVA followed by Tukey's post hoc test. Colors represent comparison to WT, and pairwise comparisons are shown with brackets and asterisks. Nonsignificant is NS (blue) and $P <$ 0.0001 is **** (green). Error bars represent SD. Scale bars: 5 AAm.

significantly higher than the single mutants (20% for *rcy1*Δ and 30% for *vps35*Δ), suggesting that both pathways are used together to recycle Dnf2 (Figure 2B). Curiously, Dnf2-mNG was highly concentrated in one or two spots on the limiting membrane of the vacuole that stained with FM4-64 in *rcy1*Δ cells, consistent with a prevacuolar compartment localization. Loss of either one of the retromer SNX or SNX-BAR components, Snx3 or Vps17, led to mislocalization of Dnf2 to the vacuole, further supporting the crucial role of retromer in localizing Dnf2 (Supplemental Figure S3). In addition, *rcy1*Δ or *vps35*Δ deletions reduced Dnf2 localization to the PM (Supplemental Figure S4). Interestingly, deletion of Snx3 or Vps17 did not cause a reduction in PM localization, even though a significant percentage of Dnf2 was mislocalized to the vacuole in these cells. The *rcy1*Δ*vps35*Δ and *snx4*Δ*vps35*Δ double mutants both showed loss of PM localization of Dnf2, consistent with its substantial mislocalization to the vacuole (Supplemental Figure S3 and S4). Thus, both retromer complexes and Rcy1 contribute to Dnf2 recycling.

We next examined Drs2 and Neo1, two Golgi localized flippases, and found the localization of Drs2 is also dependent on retromer as the *vps35*Δ deletion led to vacuolar localization (Figure 3). Similar to Dnf2, *rcy1*Δ caused a minor degree of Drs2 vacuolar mislocalization and *snx4*Δ was not significantly different from wild-type (WT). A significant percentage of Drs2 was mislocalized in the *rcy1*Δ*vps35*Δ and *snx4*Δ*vps35*Δ double mutants and the *rcy1*Δ*snx4*Δ*vps35*Δ triple mutant showed increased mislocalization relative to *vps35*Δ (Supplemental Figure S5). The individual loss of any of the SNX or SNX-BAR proteins did not lead to vacuolar mislocalization of Drs2. Consistent with previous findings, mNG-Neo1 is solely dependent on retromer for recycling as no mislocalization was observed in either the *rcy1*Δ or *snx4*Δ strains (Supplemental Figure S6).

AP-1 suppresses Dnf1 mislocalization in *rcy1*Δ*snx4*Δ mutant backgrounds

For loss of AP-1, it was surprising that the *rcy1*Δ*snx4*Δ*apl4*Δ triple mutant did not mislocalize Dnf1 to the vacuole even though the *rcy1*Δ*snx4*Δ double mutant showed significant Dnf1 mislocalization (Figure 4A; Supplemental Figure S1). This result suggested that loss of AP-1 suppressed the *rcy1*Δ*snx4*Δ trafficking defect. To further test this possibility, we performed a complementation test by introducing the WT *APL4* to the *rcy1*Δ*snx4*Δ*apl4*Δ background, which restored GFP-Dnf1 mislocalization to the vacuole (Figure 4, A and B). This result suggests that AP-1 promotes anterograde delivery of Dnf1 from the Golgi to endosomes, thereby placing a greater demand on the recycling pathways to prevent vacuolar mislocalization.

Loss of flippase carrier pathways leads to disruption of PE and PS plasma membrane asymmetry

To test whether disrupting P4-ATPase trafficking in the endosomal system causes changes to plasma membrane organization, the retrograde pathway mutants were subjected to duramycin and papuamide A (Pap A) toxin treatment. Duramycin binds to inappropriately exposed PE in the extracellular leaflet of the PM and creates a pore to disrupt the cell's membrane potential and cause cell death (Aoki *et al.*, 1994). Single deletions of *rcy1*Δ and *vps35*Δ were hypersensitive to duramycin relative to WT cells, indicating a loss of PE asymmetry (Figure 5, A and B). Double and triple deletions, including either *rcy1*Δ or *vps35*Δ, led to even greater

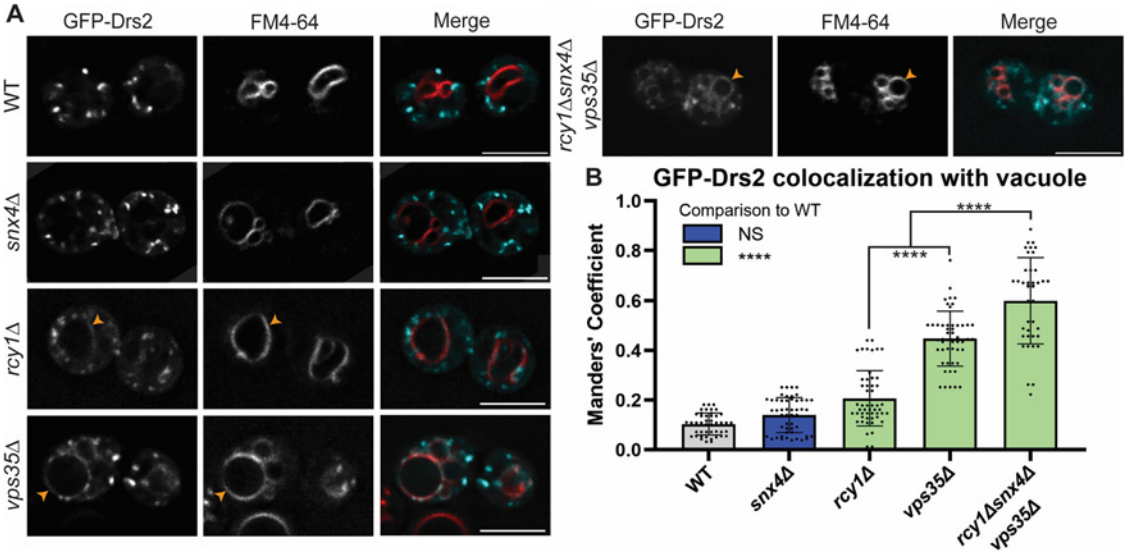

FIGURE 3: Retromer plays a major role in Drs2 recycling with a minor contribution from Rcy1. (A) Localization of GFP-Drs2 in retrograde mutants. Orange arrowheads point to GFP-Drs2 localization at the vacuole limiting membrane. (B) Quantification via Manders' coefficient of the proportion of GFP-Drs2 colocalized with FM4-64 (vacuole limiting memebrane). For all quantification, data from ~45 cells from three independent experiments were obtained and analyzed. Comparisons were calculated via a one-way ANOVA followed by Tukey's post hoc test. Colors represent comparison to WT, and pairwise comparisons are shown with brackets and asterisks. Nonsignificant is NS (blue) and $P <$ 0.0001 is **** (green). Error bars represent SD. Scale bars: 5 AAm.

sensitivity. For example, the growth of the *rcy1Δvps35Δ* double mutant was inhibited at even 2.5 AAM duramycin, whereas WT was inhibited at 40 AAM (Figure 5B). Pap A binds to inappropriately exposed PS on the PM and forms pores that disrupt membrane integrity, causing cell death (Parsons *et al.*, 2006). The *rcy1Δ* single mutant shows significant sensitivity to 1.5 AAg/ml Pap A compared with WT, and the *rcy1Δvps35Δ* double mutant was sensitive to 0.5 AAg/ml where WT is inhibited at 4.5 AAg/ml (Figure 5C). Previous work from our lab shows that loss of Neo1 temperature sensitive alleles are hypersensitive to both Pap A (IC50 2.5–3.5 AAg/ml) and duramycin (10–20 AAM) at both permissive and nonpermissive temperatures (Takar *et al.*, 2016). Deletion of Drs2 has been reported to have hypersensitivity to both Pap A (IC50 2.5–3.5 AAg/ml) and duramycin (IC50 30–40 AAM). These results show that loss of Rcy1 and retromer greatly disrupts PM asymmetry for both PE and PS, consistent with the observations that these two pathways are important for P4-ATPase localization.

The N-terminal tail of Dnf1 contains two FXFXD retromer motifs

The retromer requirement for Dnf1, Dnf2, and Drs2 localization suggests that these proteins are likely to contain sorting signals recognized by retromer. Using consensus motifs for known retromer recognition, the Pattern Matching software in the *Saccharomyces* Genome Database was used to identify any of these motifs within the cytosolic regions of the flippases. We found two potential motifs within the N-terminal tail (NT) of Dnf1 and 1 potential

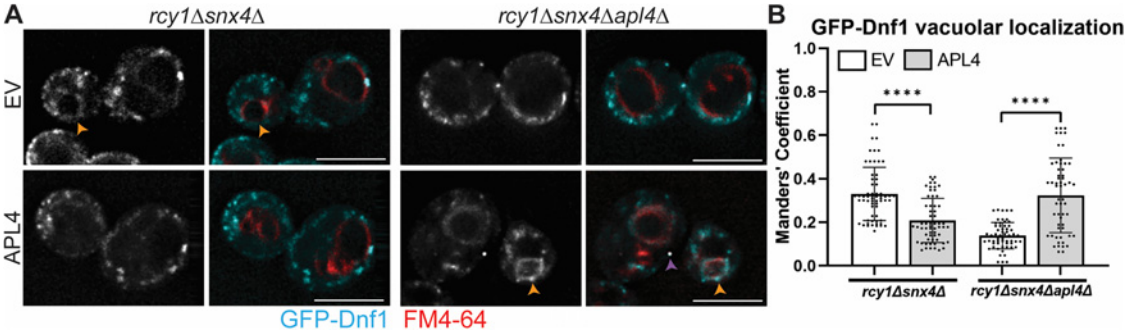

FIGURE 4: AP-1 deletion suppresses Dnf1 mislocalization in *rcy1Δsnx4Δ* mutant backgrounds. (A) Localization of GFP-Dnf1 in *rcy1Δsnx4Δ* and *rcy1Δsnx4Δapl4Δ* strains expressing WT *APL4* or an empty vector (EV). Orange arrowheads point to vacuole limiting membrane GFP-Drs2 localization. Purple arrow points to colocalized dot that is a defect of our microscope. (B) Quantification via Manders' coefficient of the proportion of GFP-Dnf1 colocalized with FM4-64 (vacuole limiting membrane). For all quantification, data from ~45 cells from three independent experiments were obtained and analyzed. Comparisons were calculated via a one-way ANOVA followed by Tukey's post hoc test. Pairwise comparisons are shown with brackets and asterisks. $P <$ 0.0001 is ****. Error bars represent SD. Scale bars: 5 AAm.

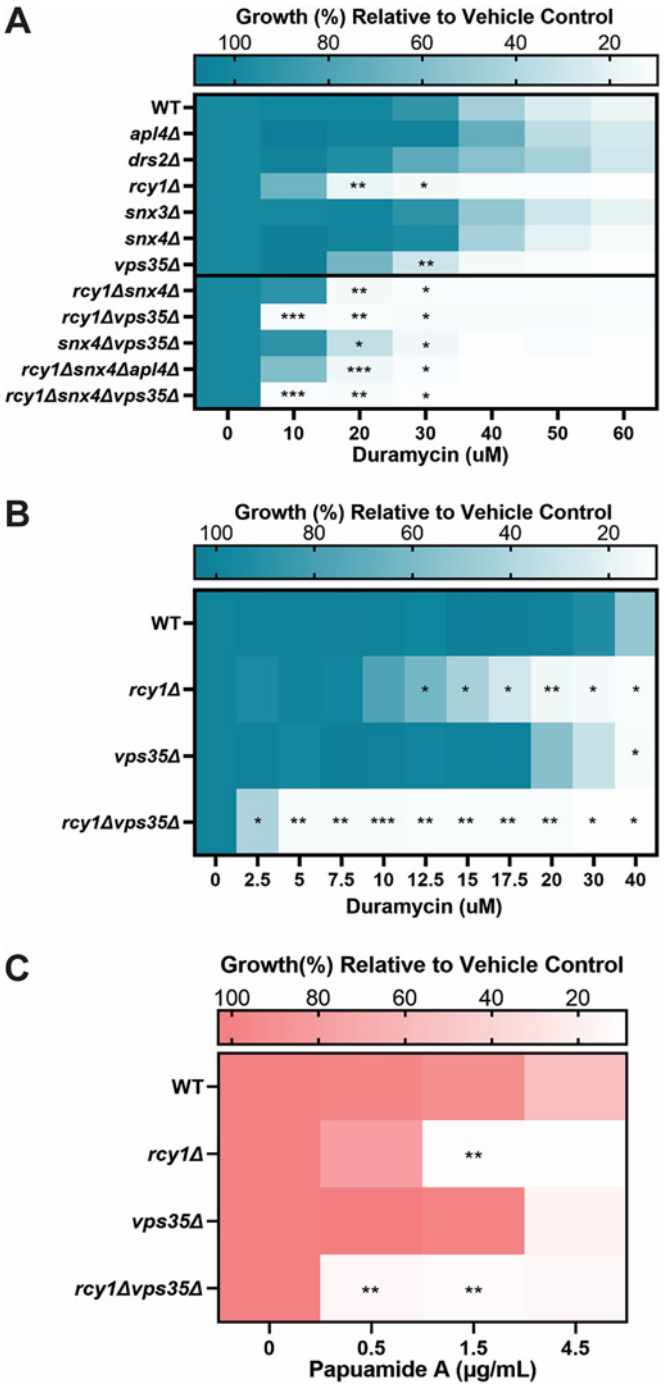

FIGURE 5: Loss of retromer and Rcy1 leads to disruption of PE and PS plasma membrane asymmetry. (A and B) The blue heat maps display duramycin dose responses at (A) 10 AAM interval concentration range and (B) a smaller 2.5 AAM interval range in the growth of yeast strains indicated. (C) The pink heat map displays Pap A dose responses at selected concentrations. The data represent growth relative to corresponding yeast strains in the absence of drug. The average of three replicates is plotted and statistical differences of each strain compared with WT at each concentration were calculated with a mixed-effect analysis followed by a Dunnett's post hoc test. $P < 0.05$ is *, $P < 0.01$ is **, $P < 0.001$ is ***.

motif in the NT of Dnf2 (Figure 6A). Drs2 contained five potential motifs in the NT, three in a cytosolic region preceding TM3, four motifs between TM6 and TM7, and three potential motifs within the C-terminal tail (CT). The known FEM motif on Neo1 was revealed in the search while no motifs were found in Dnf3 (Figure 6A). Finally, pattern matching of conserved motifs within the β-subunits of the flippases revealed a Ω-ϕ-L/M/V motif at the start of the CT of Lem3, which would not likely serve as a motif due to its membrane proximity (Supplemental Figure S7). Additionally, for Cdc50, pattern matching revealed a potential Ω-x-x-L/M/V motif within the CT, which could serve as a retromer motif (Supplemental Figure S7).

We tested the capacity of the identified motifs in Dnf1 or Dnf2 to be retromer-dependent sorting signals by fusing the NT of the flippase proteins to a known retromer cargo, Ste13, lacking its sorting signal (GFP-Dnf1-Ste13, GFP-Dnf2-Ste13; Figure 6B). Ste13 is known to cycle between the multivesicular body (MVB) and TGN and contains an FxFxD sorting motif within the cytoplasmic NT. Loss of the NT of Ste13 (S13ΔNT) and the sorting motif, leads to vacuolar localization due to loss of retromer recognition (Figure 6, C and D) (Nothwehr *et al.*, 2000). The GFP-Dnf1-Ste13 fusion protein showed a punctate localization pattern in WT cells equivalent to that of Ste13 and was mislocalized to the vacuole in *vps35*Δ cells, confirming the presence of a retromer-dependent sorting signal in the Dnf1 NT (Figure 6, C and D). However, the GFP-Dnf2-Ste13 fusion protein localized to the vacuole in WT cells, indicating the 210-YNL-212 sequence in the NT of Dnf2 is unlikely to be a retromer sorting motif.

To directly test the 20-FQFED-24 and 69-FTFND-73 motifs found in Dnf1, we created alanine mutations of the motif in the GFP-Dnf1-Ste13 construct (Figure 7A). Only the phenylalanines (F20 = F_1, F22 = F_2, F69 = F_3, F71 = F_4) were mutated because these residues were shown to be critical for Ste13 sorting by retromer (Nothwehr *et al.*, 1993). Single mutations of F_2, F_3, or F_4 led to the mislocalization of the Dnf1-Ste13 fusion protein to the vacuole (Figure 7, B and C). The F_2F_3 and F_2F_4 double mutants both showed equivalent mislocalization to the vacuole as the single mutants. This shows that both the FQFED and FTFND are retromer-dependent sorting motifs, but these motifs did not appear to be redundant as single mutations were sufficient to disrupt the localization of the fusion protein. We next tested whether the FQFED and FTFND motifs are necessary for localization by mutating these motifs in the context of full-length Dnf1. The single mutations of F_2, F_3, and F_4 did not alter the localization of Dnf1 nor did the double mutations F_2F_3 and F_2F_4 (Figure 7D). These results either indicate that FQFED and FTFND are not recognized by retromer in the context of the full-length protein or that additional retromer motifs are present in Dnf1.

The CTs of Dnf1 and Dnf2 contain a novel retromer-dependent signal

The Dnf1 and Dnf2 CT lacked any known retromer motifs. Therefore, we tested for the presence of a novel motif by creating fusion proteins between the known retromer cargo Vps10 and the full-length CTs (100%CT) of both Dnf1 and Dnf2 (Figure 8A). Vps10 is a vacuolar hydrolase sorting receptor that localizes to the MVB and TGN as it delivers its cargo and gets recycled back (Figure 8B; Seaman *et al.*, 1997). Vps10 contains two retromer motifs FGEIRL and YSSL (Cooper and Stevens, 1996; Suzuki *et al.*, 2019) in the CT of the receptor and loss of the CT (Vps10ΔCT) leads to vacuolar localization (Figure 8B). The Vps10-Dnf1-100%CT-GFP and Vps10-Dnf2-100%CT-GFP fusion proteins displayed punctate

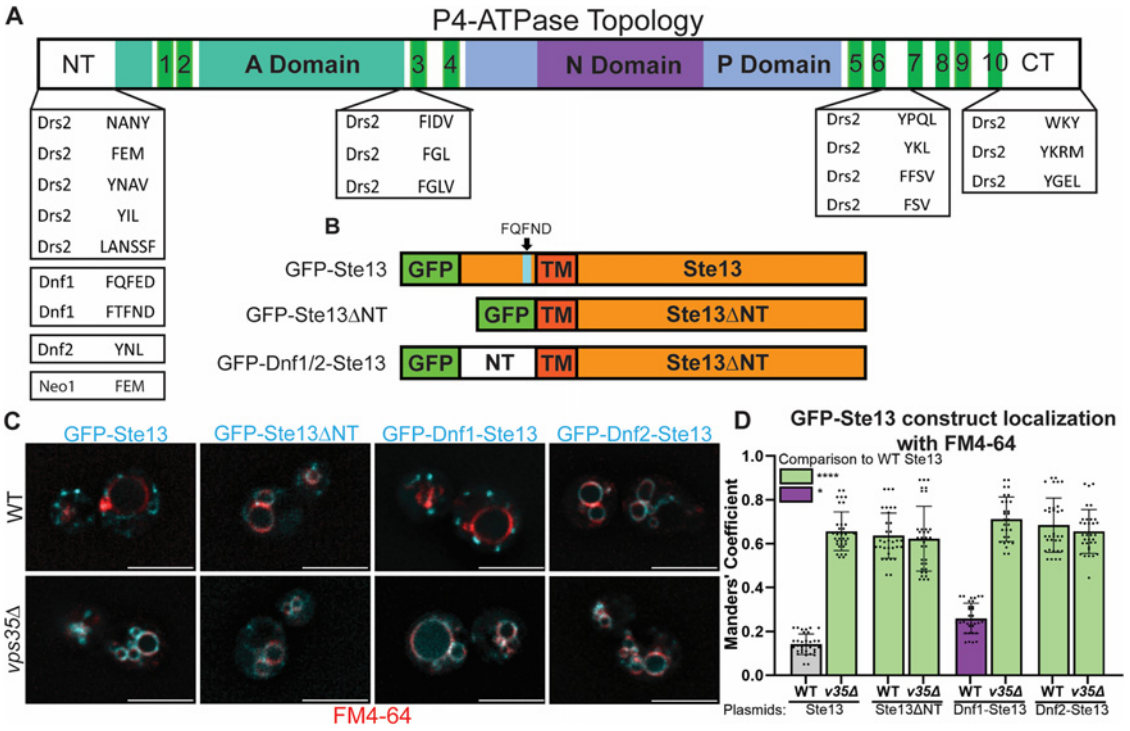

FIGURE 6: The NT of Dnf1 contains a retromer sorting motif while the Dnf2 NT lacks a recycling signal. (A) Topology of the P4-ATPases with results from the retromer motif pattern matching searches for all the flippases. Dnf3 does not contain any predicted motifs. Bright green labels each transmembrane domain. Other domains are labeled as indicated. (B) Schematic of the Ste13 and the flippase-Ste13 fusion proteins. Orange is Ste13 components, blue signifies the known retromer motif, and white represents flippase components. (C) Localization of GFP-Ste13, GFP-Ste13ΔNT, and GFP-flippase-Ste13ΔNT fusion proteins in WT and *vps35*Δ backgrounds. (D) Quantification via Manders' coefficient of the proportion of GFP-tagged cargo colocalized to FM4-64 (vacuole limiting memebrane). For all quantification, data from ~30 cells from three independent experiments were obtained and analyzed. Comparisons calculated via a one-way ANOVA followed by Tukey's post hoc test. Colors represent a comparison to WT. $P < 0.05$ is * (purple) and $P < 0.0001$ is **** (green). Error bars represent SD. Scale bars: 5 AAm.

localization in WT cells and vacuolar localization in *vps35*Δ, indicating that retromer can recognize the CT of both Dnf1 and Dnf2 (Figure 8, C–F). To narrow down where the motif is found within the 179/178 amino acid CT of Dnf1/Dnf2, we created stepwise truncations from the C-terminus, thereby reducing the full-length CT by 25% with each truncation (Figure 8A; see Supplemental Table S2 for the Dnf1 and Dnf2 amino acid numbers present in each construct). We found that both the Vps10-Dnf1-50%CT-GFP and the Vps10-Dnf1-75%CT-GFP showed normal MVB/TGN localization while the Vps10-Dnf1-25%CT-GFP fusion protein had vacuolar localization (Figure 8, C and D). Similarly, the Vps10-Dnf2 truncated constructs showed the same pattern (Figure 8, E and F). The full-length and truncated fusion proteins displayed a minor mislocalization to the lumen of the vacuole; therefore, we quantified colocalization of the fusion constructs with the luminal marker CMAC. The pattern of construct mislocalization to the vacuole was consistent between the CMAC and FM4-64 colocalization data (Supplemental Figure S8). These results indicated that the 25–50% interval of the CT for both proteins contains a retromer-dependent sorting signal.

An alignment of the 25–50% interval from both Dnf1 and Dnf2 revealed a conserved 1468/1510-VTEEIPM[TS]-1475/1517 sequence (Figure 9A; Dnf1/Dnf2 locations, respectively). To test this VTEEIPM[TS] sequence, we created alanine mutations of the TEE and IPM[TS] in the Vps10-Dnf1 and Vps10-Dnf2 fusion proteins. The mutation of TEE>AAA in Vps10-Dnf1 and Vps10-Dnf2 did not cause mislocalization of either protein to the limiting membrane or lumen of the vacuole, indicating the TEE is not a retromer-dependent sorting signal (Figure 9B; Supplemental Figure S8). In contrast, the mutation of IPM[TS]>AAAA led to mislocalization of both fusion proteins to the vacuole, implying that the IPM[TS] is a novel retromer-dependent sorting signal (Figure 9C; Supplemental Figure S8). We further tested which amino acids may play a key role in retromer-dependent sorting by mutating each amino acid to alanine. We found that the Vps10-Dnf1 I1472A and M1474A mutants showed partial mislocalization to the limiting membrane and lumen of the vacuole, demonstrating an important role of these residues (Figure 9D; Supplemental Figure S9). Additionally, the M1517A mutation in the Vps10-Dnf2 protein caused slight mislocalization to the limiting membrane and lumen of the vacuole, also implying an important role in the interaction (Figure 9E; Supplemental Figure S9). We next tested the requirement for the IPMT motif in the sorting of full-length Dnf1. Mutations of IPMT>AAAA in Dnf1 did not affect the localization of the protein, presumably because retromer was still able to bind to the two N-terminal motifs (Figure 9F).

Dnf1 uses three retromer sorting motifs for proper localization

To test whether both the NT and CT motifs contributed to Dnf1 sorting, we created various combinations of each FQFED (F_1F_2), FTFND (F_3F_4), and IPMT motif mutation in the full-length Dnf1. We found that the FQFED and IPMT combination of mutations did not

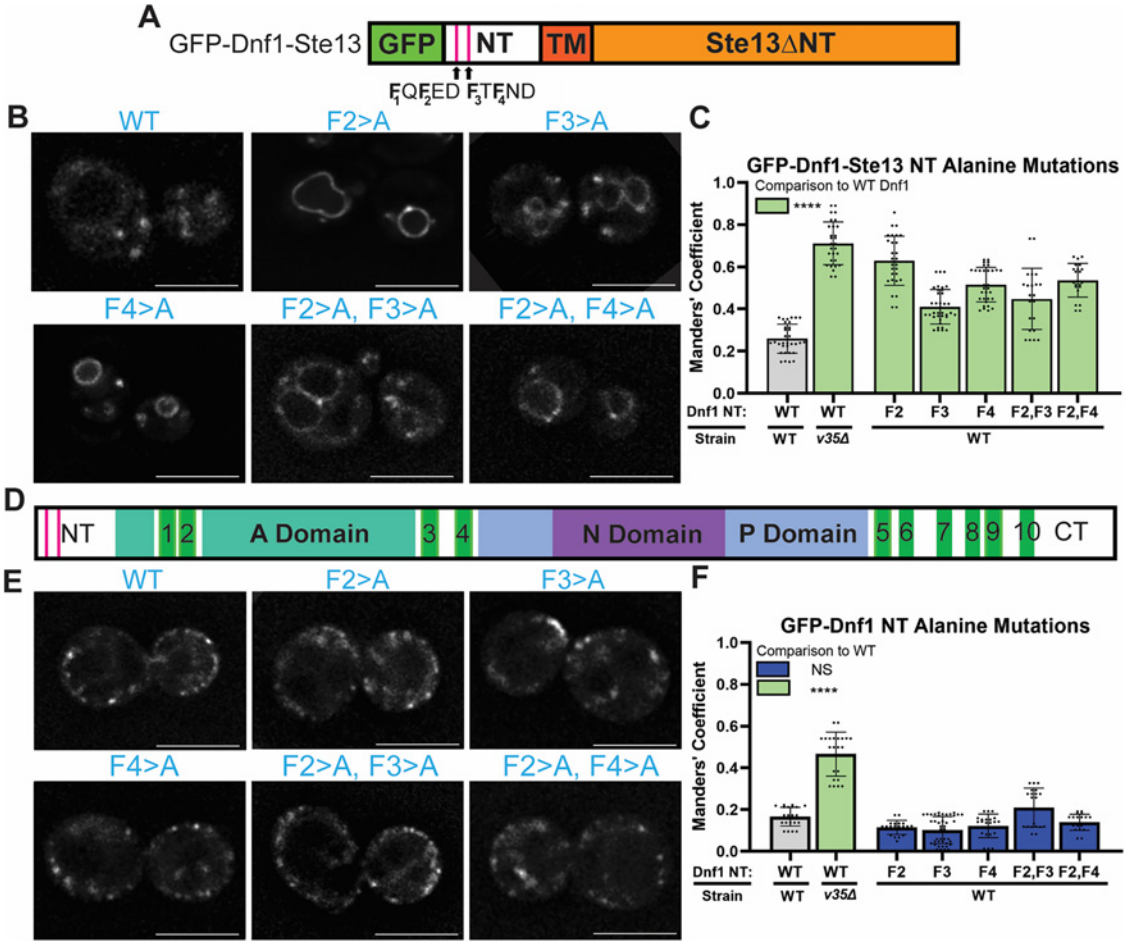

FIGURE 7: Mutation of FQFED and FTFND motifs disrupts retromer-dependent recycling of GFP-Dnf1-Ste13 but not GFP-Dnf1. (A) Schematic of the GFP-Dnf1-Ste13 fusion protein with pink labeling FQFED and FTFND motifs. Each phenylalanine is numbered and F>A corresponds to single alanine substitutions as indicated. (B) Localization of GFP-Dnf1-Ste13 fusion protein mutants. (C) Quantification via Manders' coefficient of the proportion of GFP-Dnf1-Ste13 mutants colocalized with FM4-64 (vacuole limiting membrane). (D) Schematic of GFP-Dnf1 protein with noted FQFED and FTFND motifs in pink. (E) Localization of GFP-Dnf1 with phenylalanine mutations. (F) Quantification via Manders' coefficient of the proportion of GFP-Dnf1 mutants colocalized to FM4-64 (vacuole limiting membrane). For all quantification, data from ~30 cells from three independent experiments were obtained and analyzed. Comparisons were calculated via a one-way ANOVA followed by Tukey's post hoc test. Colors represent comparisons to WT. Nonsignificant is NS (blue) and $P < 0.0001$ is **** (green). Error bars represent SD. Scale bars: 5 AAm.

mislocalize Dnf1 to the vacuole while the combination of FTFND and IPMT mutations did (Figure 10, B and C). Mutation of the FQFED, FTFND, and IPMT motifs caused further mislocalization of Dnf1 to the vacuole, greater than that of the double mutant (Figure 10, B and C). This result suggests that both the NT and CT of Dnf1 and all three retromer-dependent signals contribute to Dnf1 recycling (Supplemental Figure S10). Furthermore, the FQFED, FTFND, and IPMT mutant motifs expressed in *vps35*Δ showed equivalent mislocalization to the triple mutant in the WT background (Figure 10C). Thus, there does not appear to be any more retromer-dependent signals in Dnf1, and the predicted signal in the Lem3 CT does not appear to be used.

DISCUSSION

In this study, we describe the endosomal recycling pathways traveled by four of the five of the P4-ATPases in *S. cerevisiae*, modeled in Figure 10D. We show that Dnf1, Dnf2, Drs2, and Neo1 all require retromer for normal localization to the Golgi and/or plasma membrane. The Rcy1 pathway contributes significantly to Dnf1, Dnf2, and Drs2 recycling, while only Dnf1 was missorted in cells lacking Snx4. The observation that several P4-ATPases use multiple modes of recycling indicates that as the flippase cargos move through the endocytic pathway, there are many opportunities for incorporation into a carrier for delivery to the Golgi. However, it should be noted that the *rcy1*Δ*snx4*Δ*vps35*Δ triple mutant does not completely mislocalize any of the P4-ATPases to the vacuole. This could be due to a slow movement of these cargos into the endosomal system relative to proteins like Vps10, or that additional trafficking pathways are operating to recycle the P4-ATPases. One unexplored endosomal recycling pathway is mediated by the PX-BAR protein Mvp1, which recycles Vps55 and Nhx1 out of the multivesicular body (Suzuki *et al.*, 2021). Further studies will be needed to investigate any potential role Mvp1 has on P4-ATPase localization. However, it is clear that retromer plays the dominant role in retrieving P4-ATPases from endosomes; therefore, these cargos must have retromer-dependent sorting signals.

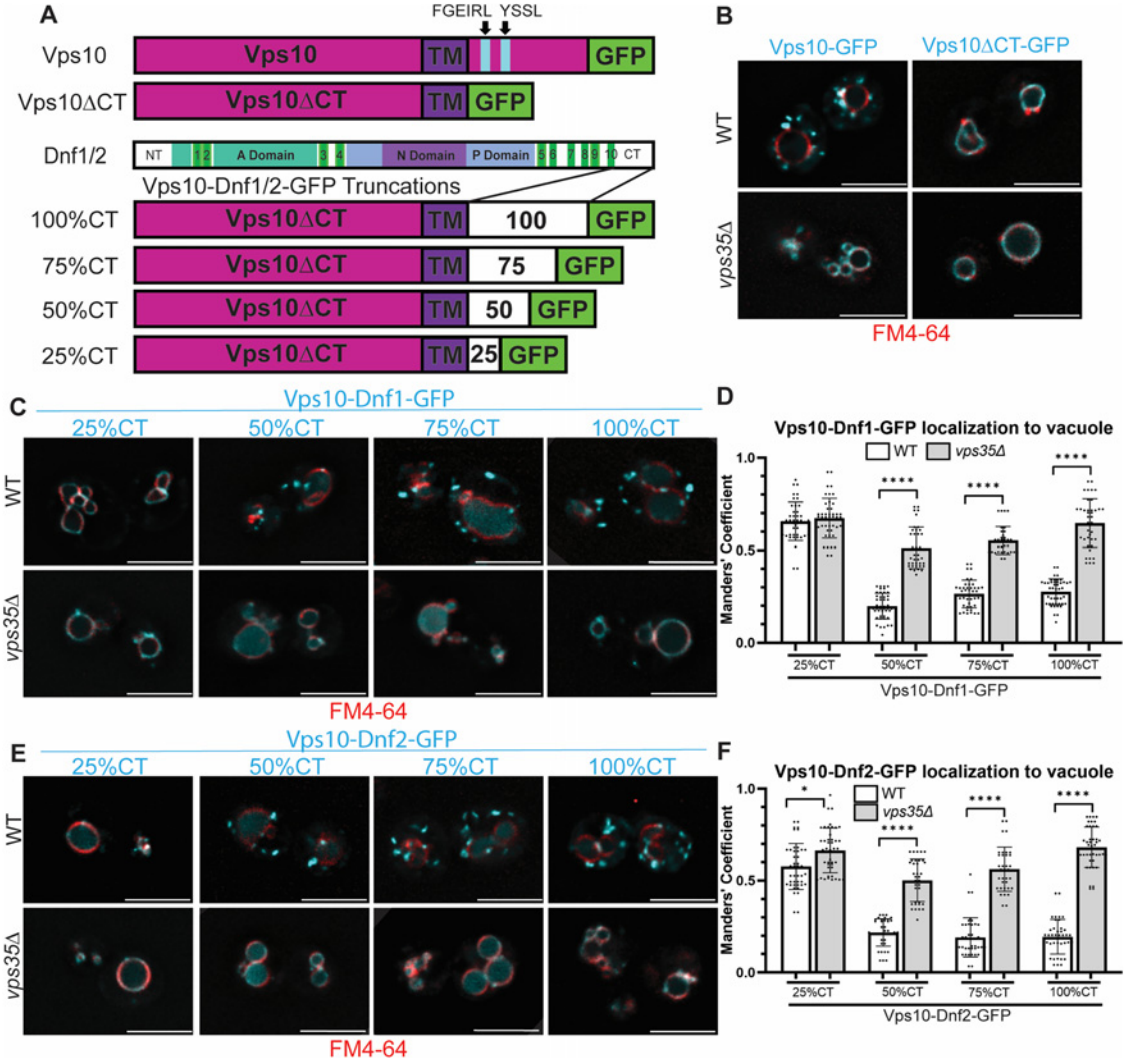

FIGURE 8: The CTs of Dnf1 and Dnf2 contain a retromer sorting motif. (A) Schematic of Vps10-GFP and Vps10ΔCT-GFP. The Dnf1/Dnf2 topology is show as well as the Vps10-Dnf1/2-GFP fusion proteins with either 100%, 75%, 50%, or 25% truncations from the C-terminal side. Purple is the Vps10 component, blue indicates known retromer motifs, and white represents flippase components. (B) Localization of Vps10-GFP and Vps10ΔCT-GFP in WT and *vps35*Δ. (C and D) Localization and quantification of Vps10-Dnf1-GFP and listed truncations. (E and F) Localization and quantification of Vps10-Dnf2-GFP and listed truncations. For all quantification, data from ~45 cells from three independent experiments were obtained and analyzed. Comparisons were calculated via a one-way ANOVA followed by Tukey's post hoc test. Pairwise comparisons are shown with brackets and asterisks. $P < 0.0001$ is ****. Error bars represent SD. Scale bars: 5 AAm.

We found a large number of potential retromer-dependent sorting signals in the P4-ATPases and discovered that IPM[TS] is a novel retromer-dependent sorting motif in the CT of Dnf1 and Dnf2. For other known retromer-dependent signals, large aromatic amino acids (FYW), charged amino acids (DE), and hydrophobic amino acids (ILMV) can all be included where the aromatic and hydrophobic residues are typically required. The IPM[TS] motif contains a pair of hydrophobic residues important for function (I and M) but lacks a bulky aromatic residue present in all other retromer motifs. The conserved proline is an unusual amino acid to be present as it would constrain the flexibility of the peptide, but a proline to alanine substitution did not disrupt its function. Strochlic and Burd (2007) identified a retromer-dependent sorting signal in the CT of Frt1, which was mapped to a nine amino acid region. This Ftr1 region contains an LPFT sequence that is similar to the IPM[TS] signal in Dnf1 and Dnf2, suggesting that the novel retromer-dependent signal could be defined as [IL]P[MF][TS]. However, further studies are needed to determine whether the Ftr1 LPFT sequence is required for its retromer-dependent sorting and to determine the full range of amino acid sequences that comprise this sorting signal.

Along with the newly discovered CT motif, Dnf1 also contains two NT FxFxD motifs. Unexpectedly, the FQFED and FTFND motifs are not redundant with each other in the context of GFP-Dnf1-Ste13 as single mutations caused mislocalization of the fusion protein. However, in full-length Dnf1, triple mutation of both FXFXD motifs and the IPM[TS] is required for the greatest extent of vacuolar mislocalization, equivalent to what is observed for WT Dnf1 in *vps35*Δ cells. The FXFXD and IPM[TS] motifs are in unstructured regions of Dnf1 and Dnf2 based on available cryoEM structures and AlphaFold predictions (Supplemental Figure S10) (Bai *et al.*, 2020;

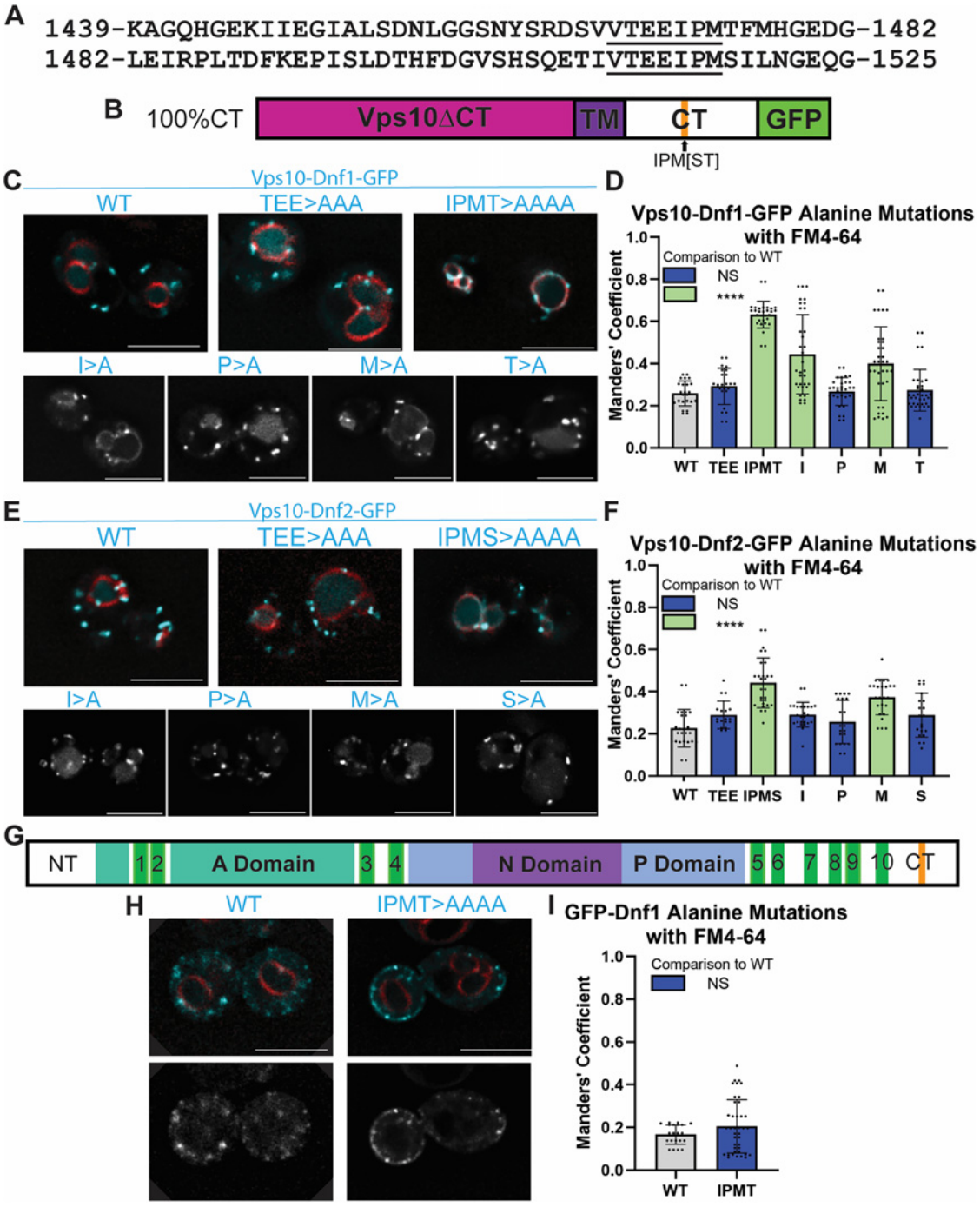

FIGURE 9: The CTs of Dnf1 and Dnf2 contain a novel IPM[TS] retromer-dependent sorting motif. (A) Sequence alignment of the 25–50% interval for the Dnf1 CT and Dnf2 CT. (B) Construct used for mutation of potential sorting signals with IPM[TS] motif indicated in orange. (C–F) Localization and quantification of Vps10-Dnf1-GFP (C,D) and Vps10-Dnf2-GFP (E,F) alanine mutation variants in WT cells. (G) Position of IPMT in the Dnf1 construct is indicated in orange. (H and I) Localization and quantification of GFP-Dnf1 CT mutant. Mutation of IPMT to AAAA does not cause Dnf1 mislocalization to the vacuole. For all quantification, data from ~30 cells from three independent experiments were obtained and analyzed. Comparisons were calculated via a one-way ANOVA followed by Tukey's post hoc test. Colors represent comparisons to WT. Nonsignificant is NS (blue) and P <0. 0001 is **** (green). Error bars represent SD. Scale bars: 5 AAm.

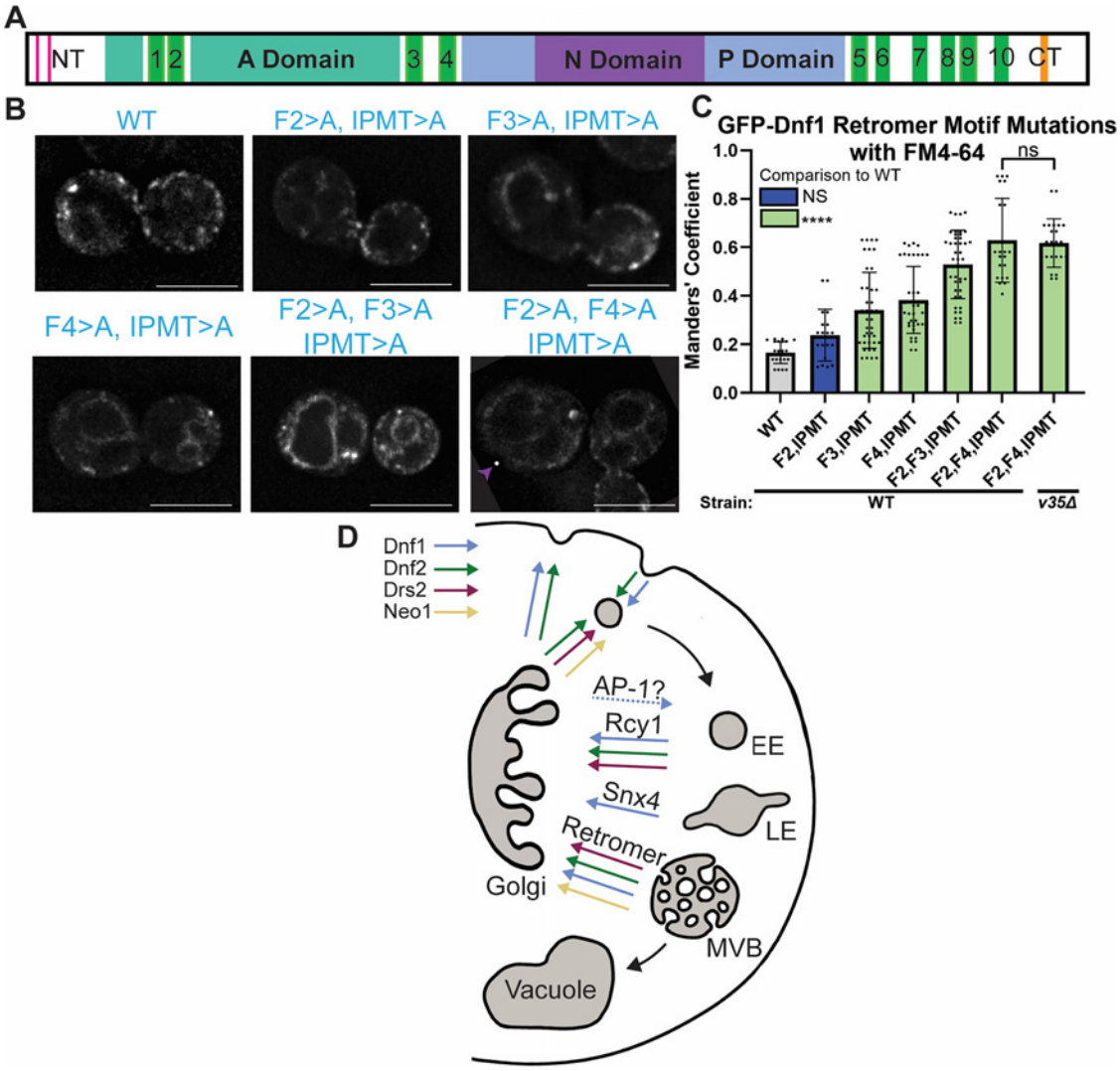

FIGURE 10: Dnf1 uses three retromer sorting motifs for endosomal recycling. (A) Dnf1 diagram with the positions of FXFXD motifs (pink) and IPMT (orange) indicated. (B and C) Localization and quantification of GFP-Dnf1 NT and CT mutations. Double and triple mutations of retromer motifs in Dnf1 cause vacuolar mislocalization. Purple arrow points to colocalized dot that is a defect of our microscope. (D) Final model for recycling pathways traveled by Dnf1 (Blue), Dnf2 (Green), Drs2 (Maroon), and Neo1 (Yellow). Dashed arrow indicated uncertainty. EE – early endosome, LE – late endosome, MVB – multivesicular body. For all quantification, data from ~30 cells from three independent experiments were obtained and analyzed. Comparisons were calculated via a one-way ANOVA followed by Tukey's post hoc test. Colors represent comparisons to WT. Nonsignificant is NS (blue) and $P < 0.0001$ is **** (green). Error bars represent SD. Scale bars: 5 AAm.

Jumper *et al.*, 2021; Varadi *et al.*, 2022) (AlphaFold Database: P32660 and Q3MRI3). Thus, mutations in these sequences are unlikely to perturb the folding or catalytic function of the P4-ATPase. Consistently, the Dnf1 mutants exit the ER efficiently, indicating that they can fold properly and form heterodimers with Lem3, their noncatalytic β-subunit. Dnf1 is the only retromer cargo we are aware of with functionally defined retromer-dependent sorting signals in both a C-terminal and N-terminal cytosolic tails (Supplemental Figure S10). This could speak to the importance of shuttling Dnf1 to its correct location, similar to Drs2 and its large number of predicted motifs. Lem3 also contains a potential retromer sorting motif, although it is very close to the transmembrane segment and does not appear to contribute to Dnf1-Lem3 sorting. Furthermore, Cdc50 appears to contain a classical retromer motif, but further testing will need to be performed to confirm this.

In budding yeast, the core retromer complex (Vps35-Vps29-Vps26) appears to interact with Snx3 homodimers or Vps5-17 heterodimers in a mutually exclusive manner (Simonetti and Cullen, 2018; Kovtun *et al.*, 2018). Both Snx3-Snx3 and Vps5-Vps17 dimers contain the PI3P-binding PX domain allowing for membrane sensing, while Vps5 and Vps17 both contain a BAR domain capable of bending the membrane. While some cargoes can use either Snx3-retromer or Vps5/17-retromer (Voos and Stevens, 1998; Hettema *et al.*, 2003), some distinct cargoes, such as Ste13 and Neo1, appear to be solely recognized by Snx3-retromer (Strochlic *et al.*, 2007; Dalton *et al.*, 2017). Ste13 has an FXFXD motif recognized by Snx3-retromer, comparable to the two motifs in the Dnf1 NT. Similarly, Ftr1 contains the [IL]P[MF][TS] and primarily relies on Snx3-retromer for recycling (Strochlic *et al.*, 2007). However, Dnf1 shows strong mislocalization when Vps5 or Vps17 is deleted, and only

slight mislocalization with the loss of Snx3. Thus, it is likely that Vps5/17-retromer recognition of the N- and C-terminal signals is primarily used to traffic Dnf1. How cargos are distinguished by Vps5/17-retromer and Snx3-retromer remains unclear. However, the stage of endosome maturation may play a more prominent role than the specific sorting signals in determining which retromer complex is used for recycling. The loss of either Snx3 or Vps17 leads to the mislocalization of Dnf2, further complicating the relationship between the sorting signals and the sorting nexins. Drs2 has 15 potential retromer-dependent localization signals and localizes normally in either *snx3*Δ, *vps5*Δ, or *vps17*Δ individual mutants. Thus, it appears that retromer can use any one of the sorting nexin complexes to sort Drs2 efficiently. Drs2 could also potentially use Atg18-retromer for sorting, but further studies are needed to parse out the role of Atg18-Retromer in Drs2 trafficking (Krick *et al.*, 2008; Courtellemont *et al.*, 2022; Marquardt *et al.*, 2023). It is still unknown whether the sorting nexins are able to directly identify and select for cargo. There is structural evidence for Snx3 interacting with the cargo once the Vps26-Vps35-Vps29 trimer has been recruited, while it is thought the trimer core in Vps5/17-retromer selects the cargo (Lucas *et al.*, 2016; Tu and Seaman, 2021).

The AP-1 clathrin adaptor does not appear to play a role in the retrograde transport of P4-ATPases from endosomes. We found no evidence that AP-1 deficiency caused mislocalization of any P4-ATPase to the vacuole. We have previously shown that AP-1 mutants substantially enhance the rate of Drs2 transport from the Golgi to the plasma membrane, but Drs2 is rapidly endocytosed and efficiently recycled back to the Sec7-marked late Golgi compartment in the absence of AP-1. We proposed that AP-1/clathrin vesicles containing Drs2 were either targeted to an early endosome (anterograde function) or to earlier Golgi compartments (intra-Golgi retrograde function) (Liu *et al.*, 2008). More recent studies also suggested that AP-1 mediates intra-Golgi retrograde transport of Drs2 (Casler *et al.*, 2019, 2022). Here, we show that vacuolar mislocalization of Dnf1 and Dnf2 observed in *rcy1*Δ*snx4*Δ double mutant is strongly suppressed in the *rcy1*Δ*snx4*Δ*apl4*Δ triple mutant. Readdition of *APL4* to the triple mutant restored the Dnf1 vacuolar mislocalization phenotype. This result suggests that Dnf1 and Dnf2 are also cargoes of AP-1/Clathrin vesicles targeted to endosomes and the *presence* of AP-1 increases the flux of these proteins into the endosomes (Figure 10D), thereby placing a greater demand on endosome to Golgi recycling pathways to prevent mislocalization to the vacuole. If AP-1 mediates intra-Golgi retrograde transport of Dnf1 and Dnf2, one would expect that the *absence* of AP-1 would increase flux into endosomes leading to increased vacuolar localization in *rcy1*Δ*snx4*Δ*apl4*Δ cells, but the opposite result was observed. Therefore, we suggest that AP-1 primarily mediates P4-ATPase transport from the Golgi to endosomes. These results also suggest a more complex trafficking itinerary for Dnf1 and Dnf2 than we expected. Rather than a single Golgi → plasma membrane → endosome → Golgi cycle, some fraction of these proteins appears to cycle between the Golgi and endosomes without necessarily trafficking to the plasma membrane.

An important discovery culminating from this work is the extensive involvement of the Rcy1 pathway for trafficking the P4-ATPases (Figure 10D). We previously found that Rcy1 functions with Drs2 and COPI in the ubiquitin-dependent recycling of a SNARE protein (Xu *et al.*, 2017; Best *et al.*, 2020). The primary function of Rcy1 in this pathway appears to be the activation of Drs2 (Hanamatsu *et al.*, 2014). Rcy1 binds to the autoinhibitory C-terminus of Drs2 along with phosphatidylinositol-4-phosphate and the ArfGEF Gea2, and these interactions activate Drs2 to promote the development of membrane curvature and a negatively charged cytosolic leaflet (Chantalat *et al.*, 2004; Natarajan *et al.*, 2009; Xu *et al.*, 2013). Here, we show that Drs2, Dnf1, and Dnf2 are partially mislocalized in *rcy1*Δ cells, but it was surprising that *drs2*Δ mutants did not show the same degree of Dnf1 or Dnf2 mislocalization as was observed in *rcy1*Δ. However, loss of Drs2 not only disrupts trafficking in the Rcy1 pathway but also the AP-1/clathrin pathway. As described above, disruption of AP-1 suppresses *rcy1*Δ*snx4*Δ trafficking defects and similarly, we suggest that loss of Drs2 reduces flux of Dnf1 and Dnf2 into the endosomes, thus allowing retromer to more effectively handle the traffic in the absence of Drs2/Rcy1 function. Dnf2 localization in *rcy1*Δ is interesting because it is concentrated at the prevacuolar compartment rather than dispersed throughout the vacuole limiting membrane. This may be attributed to Rcy1 playing an important role in the fusion of the prevacuolar compartment to the vacuole, or may suggest that Snx4 is capable of retrieving Dnf2 from the vacuole limiting membrane in this strain and delivering it to the prevacuolar membrane. Neither Dnf1 or Drs2 displays significant localization to the prevacuolar compartment in *rcy1*Δ, arguing against a general defect in fusion of this compartment with the vacuole, and suggesting that Dnf2 has a signal that allows its retrieval from the vacuole limiting membrane. In contrast, Neo1 appears to solely use retromer as a mode of endosomal recycling.

A functional consequence of P4-ATPase mislocalization in endosomal recycling mutants is the loss of the plasma membrane asymmetry and susceptibility to pore-forming toxins that target exposed PS and PE. The observation that the *rcy1*Δ mutant is more sensitive to these toxins than retromer mutants is likely because Rcy1 is an allosteric regulator of Drs2 flippase activity. The *rcy1*Δ *vps35*Δ double mutant is extremely sensitive to pap A and duramycin indicating a substantial loss of PS and PE asymmetry, consistent with the more severe P4-ATPase trafficking defect in this mutant. Membrane asymmetry in mammalian cells is tightly regulated and used to signal whether cells are living or dying. During apoptosis, activated caspases inactivate PS flippases and turn on a phospholipid scramblase (Xkr8) to allow exposure of PS in the outer leaflet (Segawa and Nagata, 2015; Nagata *et al.*, 2016; Sakuragi and Nagata, 2023). The exposed PS is an "eat me" signal that promotes recognition and phagocytosis of the cell corpses. Inappropriate exposure of PS on the surface of living, nonapoptotic cells can lead to their removal by phagocytosis and this process is thought to underlie the severe neurological and immunological diseases associated with P4-ATPase deficiency (Siggs *et al.*, 2011; Onat *et al.*, 2012; Segawa *et al.*, 2021; Meng *et al.*, 2023). If mammalian P4-ATPases display the same dependency on retromer for their functional localization as the yeast P4-ATPases, cells deficient for retromer would expose PS and could potentially be subject to nonapoptotic cell clearance. Retromer deficiency is linked to both Parkinson's and Alzheimer's diseases (Small *et al.*, 2005; Vilariño-Güell *et al.*, 2011; Zimprich *et al.*, 2011; Lane *et al.*, 2012), and it will be an important line of study moving forward to determine whether perturbation of neuronal membrane organization contributes to disease progression.

MATERIALS AND METHODS

Request a protocol through *Bio-protocol*.

Yeast strains and manipulation

The *S. cerevisiae* strains used in this study are listed in Supplemental Table S1. Standard protocols were used for yeast manipulation (Sherman, 2002). Cells were cultured at 30°C to mid-log phase in

YPD medium or SMD medium supplemented with appropriate nutrients. Yeast transformations were performed using the standard LiAc-PEG method (Gietz and Schiestl, 2007). Genomic tagging was performed using the Longtine method (Longtine, 1998).

Plasmid construction

The plasmids used in this study are listed in Supplemental Table S2 and many have been described previously (Sikorski and Hieter, 1989; Chen *et al.*, 2006; Liu *et al.*, 2007; Baldridge and Graham, 2012; Suzuki *et al.*, 2019; Jain *et al.*, 2020). pRS416-mNG-Neo1 was created via PCR amplification of *NEO1* ORF (nucleotide 1–3456 of ORF) with XhoI and ClaI restriction sites added, then restriction digestion and ligation into the pRS416-ADH-mNG plasmid. Unless otherwise specified, the remainder of the constructs were generated via Gibson assembly (New England BioLabs). All primers used for Gibson assemblies ensured a 45 bp sequence overlap between each vector end and the ends of the inserts. pRS416-GFP-Ste13 was constructed using primers for the Ste13 ORF (fragment) and pRS416-*PRC1*$_{prom}$GFP (pGO-GFP; Stefan *et al.*, 2002). The forward primer started amplification at Met1 of Ste13 and the reverse primer ended at Leu931. The fragment was inserted 10 codons downstream of GFP to N-terminally tag Ste13. pRS416-GFP-ΔNTSte13 was created by amplifying all of pRS416-GFP-Ste13 except the sequences encoding the NT, followed by blunt end ligation (NEB). pRS416-GFP-ΔNTSte13 primers were made for the GFP-Ste13 linker upstream of Met1 in Ste13 and downstream of Lys117, approximately where the transmembrane domain begins. pRS416-GFP-Dnf1-Ste13 was constructed using primers for the Dnf1 NT (Ser2-Asp216 in GFP-Dnf1 plasmid) and inserted into GFP-ΔNTSte13 directly upstream of Lys117. pRS416-GFP-Dnf2-Ste13 was constructed using primers for the Dnf2 NT (Ser2-Glu252 in pRS313-Dnf2) and GFP-ΔNTSte13 directly upstream of Lys117. pRS416-Vps10-Dnf1-GFP was constructed using primers for the Dnf1 CT (Arg1392-Asp1570 in GFP-Dnf1 plasmid) and Vps10ΔCT-GFP directly downstream of Gly1416. Primers for Dnf1 CT 25%, 50%, and 75% truncations for fragment positions as follow Arg1392-Thr1437, Arg1392-Gly1482, and Arg1392-Ser1525, respectively. pRS416-Vps10-Dnf2-GFP was constructed using primers for the Dnf2 CT (Phe1437-Arg1612 in 313-Dnf2 plasmid) and Vps10ΔCT-GFP directly downstream of Gly1416. Primers for Dnf2 CT 25%, 50%, and 75% truncations for fragment positions as follow Phe1437-Asp1481, Phe1437-Ser1525, Phe1437-Arg1569, respectively. All alanine mutations were created via Quick-Change Mutagenesis using Pfu Turbo (Agilent). Primers all have 15 bp homology flanking the alanine codon (i.e., 33 bp for single amino acid replacement).

Pattern matching search for retromer sorting motifs

The Pattern Matching software in the Saccharomyces Genome Database was used to search common yeast and mammalian retromer consensus sequences including: Ω-ϕ-L/M/V, Ω-ϕ-ϕ-L/M/V, Ω-E-F/L/M, FxFxD, ϕ-x-N-x-x-Y/F, N-x-x-Y; as well as variations of unique retromer signals such as FGEIRL (Vps10), and WKY (Stv1). Only cytoplasmic regions that are not within functional domains were searched for potential retromer sorting motifs.

Fluorescent microscopy and image analysis

To visualize fluorescent proteins within the yeast, protocols were followed as described previously (Jimenez *et. al.*, 2023). For determining the retrograde pathways traveled by Dnf1, Dnf2, Drs2, and Neo1, three biological replicates were performed with a total of ∼60 cells (20 cells per replicate) analyzed for colocalization with either vacuole limiting membrane marker FM4-64, vacuole luminal marker CMAC or plasma membrane marker Ras2-mCh. For determining the localization of flippase-reporter fusion proteins, three biological replicates for a total of ∼30 cells (10 cells per replicate) were analyzed for colocalization with FM4-64 or CMAC. Colocalization was determined through Manders' colocalization using Coloc2 in FIJI (Fiji Is Just ImageJ). Statistical analysis consisted of one-way ANOVA and Tukey's post hoc tests for multiple comparisons using GraphPad Prism v9. *P*-values of less than 0.05, 0.01, 0.001, and 0.0001 were used to show statistically significant differences and are represented with *(purple), **(orange), ***(yellow) or ****(green), respectively. *P*-values greater than 0.05 are represented by N.S. (blue).

Duramycin and Pap A sensitivity assay

For the toxin sensitivity assays, mid-log phase cells were diluted to 0.1 OD600 in fresh YPD media and 100 AAl of cells were distributed into each well of a 96-well plate. Duramycin (Sigma-Aldrich) and Pap A (a gift from Raymond Anderson from the University of British Columbia) was dissolved in DMSO and diluted to the desired concentration with fresh YPD medium. A total of 100 AAl of toxin was added to each well of the 96-well plate. Toxin dilutions were calculated to the final concentrations based on a total volume of 200 AAl/well. Plates were incubated at 30°C for 20 h. The OD600 for each well was measured using the Multimode Plate Reader Synergy HT (Biotek). Growth relative to vehicle control (only DMSO) was used as 100% growth. All values are an average of at least three biological replicates. Statistical analysis was determined using a mixed-effects analysis with significant matching (P<0.0002) followed by a Dunnett's post hoc test using GraphPad Prism v9. *P*-values of less than 0.05, 0.01, and 0.001 were used to show statistically significant differences and are represented with *, **, or ***, respectively.

Structural prediction and modeling

Models of *S. cerevisiae* Dnf1-Lem3 were generated using AlphaFold 3 using the Google DeepMind server (Abramson *et al.*, 2024). The top ranked model was visualized using UCSF ChimeraX (Goddard *et al.*, 2018; Pettersen *et al.*, 2021).

Data availability statement

The data underlying the figures are available in the published article and its online supplemental material. All analysis, original files, and reagents are available from the corresponding author upon reasonable request.

We would like to thank Scott Emr for providing the Vps10 constructs, Gregory Payne for providing the APL4 construct and Kathleen Gould for Longtine cassettes. This work was funded by 1R35GM144123 to T.R.G, 5T32MH064913 and 1F31GM150247 to M.J.

REFERENCES

Abramson J, Adler J, Dunger J, Evans R, Green T, Pritzel A, Ronneberger O, Willmore L, Ballard AJ, Bambrick J, *et al.* (2024). Accurate structure prediction of biomolecular interactions with AlphaFold 3. Nature 630, 493–500.

Alder-Baerens N, Lisman Q, Luong L, Pomorski T, Holthuis JCM (2006). Loss of P4 ATPases Drs2p and Dnf3p disrupts aminophospholipid transport and asymmetry in yeast post-Golgi secretory vesicles. Mol Biol Cell 17, 1632–1642.

Aoki Y, Uenaka T, Aoki J, Umeda M, Inoue K (1994). A novel peptide probe for studying the transbilayer movement of phosphatidylethanolamine. J Biochem 116, 291–297.

Bai L, You Q, Jain BK, Duan HD, Kovach A, Graham TR, Li H (2020). Transport mechanism of P4 ATPase phosphatidylcholine flippases. Elife 9, e62163.
Baldridge RD, Graham TR (2012). Identification of residues defining phospholipid flippase substrate specificity of type IV P-type ATPases. Proc Natl Acad Sci USA 109, E290–E298.
Bean BDM, Davey M, Conibear E (2017). Cargo selectivity of yeast sorting nexins. Traffic 18, 110–122.
Best JT, Xu P, Graham TR (2019). Phospholipid flippases in membrane remodeling and transport carrier biogenesis. Curr Opin Cell Biol 59, 8–15.
Best JT, Xu P, McGuire JG, Leahy SN, Graham TR (2020). Yeast synaptobrevin, Snc1, engages distinct routes of postendocytic recycling mediated by a sorting nexin, Rcy1-COPI, and retromer. Mol Biol Cell 31, 944–962.
Bishop WR, Bell RM (1988). Assembly of phospholipids into cellular membranes: Biosynthesis, transmembrane movement and intracellular translocation. Annu Rev Cell Biol 4, 579–610.
Bonifacino JS, Glick BS (2004). The mechanisms of vesicle budding and fusion. Cell 116, 153–166.
Burd C, Cullen PJ (2014). Retromer: A master conductor of endosome sorting. Cold Spring Harb Perspect Biol 6, a016774.
Casler JC, Johnson N, Krahn AH, Pantazopoulou A, Day KJ, Glick BS (2022). Clathrin adaptors mediate two sequential pathways of intra-Golgi recycling. J Cell Biol 221, e202103199.
Casler JC, Papanikou E, Barrero JJ, Glick BS (2019). Maturation-driven transport and AP-1–dependent recycling of a secretory cargo in the Golgi. J Cell Biol 218, 1582–1601.
Chantalat S, Park SK, Hua Z, Liu K, Gobin R, Peyroche A, Rambourg A, Graham TR, Jackson CL (2004). The Arf activator Gea2p and the P-type ATPase Drs2p interact at the Golgi in Saccharomyces cerevisiae. J Cell Sci 117, 711–722.
Chen K-E, Tillu VA, Gopaldass N, Chowdhury SR, Leneva N, Kovtun O, Ruan J, Guo Q, Ariotti N, Mayer A, Collins BM (2024). Molecular basis for the assembly of the Vps5-Vps17 SNX-BAR proteins with retromer. bioRxiv 2024.03.24.586500.
Chen S, Wang J, Muthusamy BP, Liu K, Zare S, Andersen RJ, Graham TR (2006). Roles for the Drs2p–Cdc50p complex in protein transport and phosphatidylserine asymmetry of the yeast plasma membrane. Traffic 7, 1503–1517.
Chen SH, Chen S, Tokarev AA, Liu F, Jedd G, Segev N (2005). Ypt31/32 GTPases and their novel F-box effector protein Rcy1 regulate protein recycling. Mol Biol Cell 16, 178–192.
Cooper AA, Stevens TH (1996). Vps10p cycles between the late-Golgi and prevacuolar compartments in its function as the sorting receptor for multiple yeast vacuolar hydrolases. J Cell Biol 133, 529–541.
Courtellemont T, De Leo MG, Gopaldass N, Mayer A (2022). CROP: A retromer-PROPPIN complex mediating membrane fission in the endolysosomal system. EMBO J 41, e109646.
Dalton LE, Bean BDM, Davey M, Conibear E (2017). Quantitative high-content imaging identifies novel regulators of Neo1 traffcking at endosomes. Mol Biol Cell 28, 1539–1550.
Date SS, Xu P, Hepowit NL, Diab NS, Best J, Xie B, Du J, Strieter ER, Jackson LP, Macgurn JA, Graham TR (2022). Ubiquitination drives COPI priming and Golgi SNARE localization. Elife 11, e80911.
Finnigan GC, Cronan GE, Park HJ, Srinivasan S, Quiocho FA, Stevens TH (2012). Sorting of the yeast vacuolar-type, proton-translocating ATPase enzyme complex (V-ATPase): Identification of a necessary and sufficient golgi/endosomal retention signal in Stv1p. J Biol Chem 287, 19487–19500.
Fjorback AW, Seaman M, Gustafsen C, Mehmedbasic A, Gokool S, Wu C, Militz D, Schmidt V, Madsen P, Nyengaard JR, *et al.* (2012). Retromer binds the FANSHY sorting motif in SorLA to regulate amyloid precursor protein sorting and processing. J Neurosci 32, 1467–1480.
Frøsig MM, Costa SR, Liesche J, Østerberg JT, Hanisch S, Nintemann S, Sørensen H, Palmgren M, Pomorski TG, López-Marqués RL (2020). Pseudohyphal growth in Saccharomyces cerevisiae involves protein kinase-regulated lipid flippases. J Cell Sci 133, jcs235994.
Furuta N, Fujimura-Kamada K, Saito K, Yamamoto T, Tanaka K (2007). Endocytic recycling in yeast is regulated by putative phospholipid translocases and the Ypt31p/32p-Rcy1p pathway. Mol Biol Cell 18, 295–312.
Gietz RD, Schiestl RH (2007). High-efficiency yeast transformation using the LiAc/SS carrier DNA/PEG method. Nat Protoc 2, 31–34.
Goddard TD, Huang CC, Meng EC, Pettersen EF, Couch GS, Morris JH, Ferrin TE (2018). UCSF ChimeraX: Meeting modern challenges in visualization and analysis. Protein Sci 27, 14–25.
Ha SA, Torabinejad J, DeWald DB, Wenk MR, Lucast L, De Camilli P, Newitt RA, Aebersold R, Nothwehr SF (2003). The synaptojanin-like protein Inp53/Sjl3 functions with clathrin in a yeast TGN-to-endosome pathway distinct from the GGA protein-dependent pathway. Mol Biol Cell 14, 1319–1333.
Hanamatsu H, Fujimura-Kamada K, Yamamoto T, Furuta N, Tanaka K (2014). Interaction of the phospholipid flippase Drs2p with the F-box protein Rcy1p plays an important role in early endosome to trans-Golgi network vesicle transport in yeast. J Biochem 155, 51–62.
Hettema EH, Lewis MJ, Black MW, Pelham HRB (2003). Retromer and the sorting nexins Snx4/41/42 mediate distinct retrieval pathways from yeast endosomes. EMBO J 22, 548–557.
Hua Z, Fatheddin P, Graham TR (2002). An essential subfamily of Drs2p-related P-type ATPases is required for protein trafficking between Golgi complex and endosomal/vacuolar system. Mol Biol Cell 13, 3162–3177.
Hua Z, Graham TR (2003). Requirement for Neo1p in retrograde transport from the Golgi complex to the endoplasmic reticulum. Mol Biol Cell 14, 4971–4983.
Iyoshi S, Cheng J, Tatematsu T, Takatori S, Taki M, Yamamoto Y, Salic A, Fujimoto T (2014). Asymmetrical distribution of choline phospholipids revealed by click chemistry and freeze-fracture electron microscopy. ACS Chem Biol 9, 2217–2222.
Jain BK, Roland BP, Graham TR (2020). Exofacial membrane composition and lipid metabolism regulates plasma membrane P4-ATPase substrate specificity. J Biol Chem 295, 17997–18009.
Jimenez M, Best JT, Date SS, Graham TR (2023). Quantification of golgi protein mislocalization to the budding yeast vacuole. Methods Mol Biol 2557, 17–28.
Jumper J, Evans R, Pritzel A, Green T, Figurnov M, Ronneberger O, Tunyasuvunakool K, Bates R, Žídek A, Potapenko A, *et al.* (2021). Highly accurate protein structure prediction with AlphaFold. Nature 596, 583–589.
Kato U, Emoto K, Fredriksson C, Nakamura H, Ohta A, Kobayashi T, Murakami-Murofushi K, Kobayashi T, Umeda M (2002). A novel membrane protein, Ros3p, is required for phospholipid translocation across the plasma membrane in Saccharomyces cerevisiae. J Biol Chem 277, 37855–37862.
Kovtun O, Leneva N, Bykov YS, Ariotti N, Teasdale RD, Schaffer M, Engel BD, Owen DJ, Briggs JAG, Collins BM (2018). Structure of the membrane-assembled retromer coat determined by cryo-electron tomography. Nature 561, 561–564.
Krick R, Henke S, Tolstrup J, Thumm M (2008). Dissecting the localization and function of Atg18, Atg21 and Ygr223c. Autophagy 4, 896–910.
Lane RF, George-Hyslop PS, Hempstead BL, Small SA, Strittmatter SM, Gandy S (2012). Vps10 family proteins and the retromer complex in aging-related neurodegeneration and diabetes. J Neurosci 32, 14080–14086.
Lee S, Uchida Y, Wang J, Matsudaira T, Nakagawa T, Kishimoto T, Mukai K, Inaba T, Kobayashi T, Molday RS, *et al.* (2015). Transport through recycling endosomes requires EHD1 recruitment by a phosphatidylserine translocase. EMBO J 34, 669–688.
Lewis MJ, Nichols BJ, Prescianotto-Baschong C, Riezman H, Pelham HRB (2000). Specific retrieval of the exocytic SNARE Snc1p from early yeast endosomes. Mol Biol Cell 11, 23–38.
Liu K, Hua Z, Nepute JA, Graham TR (2007). Yeast P4-ATPases Drs2p and Dnf1p are essential cargos of the NPFXD/Sla1p endocytic pathway. Mol Biol Cell 18, 487–500.
Liu K, Surendhran K, Nothwehr SF, Graham TR (2008). P4-ATPase requirement for AP-1/clathrin function in protein transport from the trans-Golgi network and early endosomes. Mol Biol Cell 19, 3526–3535.
Longtine MS, Iii K, Demarini DJ, Shah NG, Wach A, Brachat A, Philippsen P, Pringle JR (1998). Additional modules for versatile and economical PCR-based gene deletion and modification in saccharomyces cerevisiae. Yeast 14, 953–961.
Lucas M, Gershlick DC, Vidaurrazaga A, Rojas AL, Bonifacino JS, Hierro A (2016). Structural mechanism for Cargo recognition by the retromer complex. Cell 167, 1623–1635.e14.
Ma M, Kumar S, Purushothaman L, Babst M, Ungermann C, Chi RJ, Burd CG (2018). Lipid trafficking by yeast Snx4 family SNX-BAR proteins promotes autophagy and vacuole membrane fusion. Mol Biol Cell 29, 2190–2200.
MacDonald C, Piper RC (2017). Genetic dissection of early endosomal recycling highlights a TORC1-independent role for Rag GTPases. J Cell Biol 216, 3275–3290.
Marquardt L, Taylor M, Kramer F, Schmitt K, Braus GH, Valerius O, Thumm M (2023). Vacuole fragmentation depends on a novel Atg18-containing retromer-complex. Autophagy 19, 278–295.

Matsudaira T, Mukai K, Noguchi T, Hasegawa J, Hatta T, Iemura SI, Natsume T, Miyamura N, Nishina H, Nakayama J, *et al.* (2017). Endosomal phosphatidylserine is critical for the YAP signalling pathway in proliferating cells. Nat Commun 8, 1246.
McGough IJ, de Groot REA, Jellett AP, Betist MC, Varandas KC, Danson CM, Heesom KJ, Korswagen HC, Cullen PJ (2018). SNX3-retromer requires an evolutionary conserved MON2:DOPEY2:ATP9A complex to mediate Wntless sorting and Wnt secretion. Nat Commun 9, 3737.
Meng T, Chen X, He Z, Huang H, Lin S, Liu K, Bai G, Liu H, Xu M, Zhuang H, *et al.* (2023). ATP9A deficiency causes ADHD and aberrant endosomal recycling via modulating RAB5 and RAB11 activity. Mol Psychiatry 28, 1219–1231.
Nagata S, Suzuki J, Segawa K, Fujii T (2016). Exposure of phosphatidylserine on the cell surface. Cell Death Differ 23, 952–961.
Natarajan P, Liu K, Patil DV, Sciorra VA, Jackson CL, Graham TR (2009). Regulation of a Golgi flippase by phosphoinositides and an ArfGEF. Nat Cell Biol 11, 1421–1426.
Natarajan P, Wang J, Hua Z, Graham TR (2004). Drs2p-coupled aminophospholipid translocase activity in yeast Golgi membranes and relationship to in vivo function. Proc Natl Acad Sci USA 101, 10614–10619.
Nothwehr SF, Ha S-A, Bruinsma P (2000). Sorting of yeast membrane proteins into an endosome-to-Golgi pathway involves direct interaction of their cytosolic domains with Vps35p. J Cell Biol 151, 297–310.
Nothwehr SF, Roberts CJ, Stevens TH (1993). Membrane protein retention in the yeast Golgi apparatus: dipeptidyl aminopeptidase A is retained by a cytoplasmic signal containing aromatic residues. J Cell Biol 121, 1197–1209.
Onat OE, Gulsuner S, Bilguvar K, Basak AN, Topaloglu H, Tan M, Tan U, Gunel M, Ozcelik T (2012). Missense mutation in the ATPase, aminophospholipid transporter protein ATP8A2 is associated with cerebellar atrophy and quadrupedal locomotion. Eur J Hum Genet 21, 281–285.
Parsons AB, Lopez A, Givoni IE, Williams DE, Gray CA, Porter J, Chua G, Sopko R, Brost RL, Ho CH, *et al.* (2006). Exploring the mode-of-action of bioactive compounds by chemical-genetic profiling in yeast. Cell 126, 611–625.
Pettersen EF, Goddard TD, Huang CC, Meng EC, Couch GS, Croll TI, Morris JH, Ferrin TE (2021). UCSF ChimeraX: Structure visualization for researchers, educators, and developers. Protein Sci 30, 70–82.
Pomorski T, Lombardi R, Riezman H, Devaux PF, Van Meer G, Holthuis JCM (2003). Drs2p-related P-type ATPases Dnflp and Dnf2p are required for phospholipid translocation across the yeast plasma membrane and serve a role in endocytosis. Mol Biol Cell 14, 1240–1254.
Ravussin A, Brech A, Tooze SA, Stenmark H (2021). The phosphatidylinositol 3-phosphate-binding protein SNX4 controls ATG9A recycling and autophagy. J Cell Sci 134, jcs250670.
Roland BP, Graham TR (2016). Decoding P4-ATPase substrate interactions. Crit Rev Biochem Mol Biol 51, 513–527.
Roland BP, Naito T, Best JT, Arnaiz-Yépez C, Takatsu H, Yu RJ, Shin HW, Graham TR (2019). Yeast and human P4-ATPases transport glycosphingolipids using conserved structural motifs. J Biol Chem 294, 1794–1806.
Saito K, Fujimura-Kamada K, Futura N, Kato U, Umeda M, Tanaka K (2004). Cdc50p, a protein required for polarized growth, associates with the Drs2p P-type ATPase implicated in phospholipid translocation in Saccharomyces cerevisiae. Mol Biol Cell 15, 3418–3432.
Sakuragi T, Nagata S (2023). Regulation of phospholipid distribution in the lipid bilayer by flippases and scramblases. Nat Rev Mol Cell Biol 24, 576–596.
Seaman MNJ, Marcusson EG, Cereghino JL, Emr SD (1997). Endosome to Golgi retrieval of the vacuolar protein sorting receptor, Vps10p, requires the function of the VPS29, VPS30, and VPS35 gene products. J Cell Biol 137, 79–92.
Sebastian TT, Baldridge RD, Xu P, Graham TR (2012). Phospholipid flippases: Building asymmetric membranes and transport vesicles. Biochim Biophys Acta 1821, 1068–1077.
Segawa K, Kikuchi A, Noji T, Sugiura Y, Hiraga K, Suzuki C, Haginoya K, Kobayashi Y, Matsunaga M, Ochiai Y, *et al.* (2021). A sublethal ATP11A mutation associated with neurological deterioration causes aberrant phosphatidylcholine flipping in plasma membranes. J Clin Invest 131, e148005.
Segawa K, Nagata S (2015). An apoptotic 'Eat Me' signal: Phosphatidylserine exposure. Trends Cell Biol 25, 639–650.
Sherman F (2002). Getting started with yeast. Methods Enzymol 350, 3–41.
Siggs OM, Arnold CN, Huber C, Pirie E, Xia Y, Lin P, Nemazee D, Beutler B (2011). The P4-type ATPase ATP11C is essential for B lymphopoiesis in adult bone marrow. Nat Immunol 12, 434–440.
Sikorski RS, Hieter P (1989). A system of shuttle vectors and yeast host strains designed for efficient manipulation of DNA in Saccharomyces cerevisiae. Genetics 122, 19–27.
Simonetti B, Cullen PJ (2018). Endosomal sorting: Architecture of the retromer coat. Curr Biol 28, R1350–R1352.
Small SA, Kent K, Pierce A, Leung C, Kang MS, Okada H, Honig L, Vonsattel J-P, Kim T-W (2005). Model-guided microarray implicates the retromer complex in Alzheimer's disease. Ann Neurol 58, 909–919.
Stefan CJ, Audhya A, Emr SD (2002). The yeast synaptojanin-like proteins control the cellular distribution of phosphatidylinositol (4,5)-bisphosphate. Mol Biol Cell 13, 542–557.
Strochlic TI, Setty TG, Sitaram A, Burd CG (2007). Grd19/Snx3p functions as a cargo-specific adapter for retromer-dependent endocytic recycling. J Cell Biol 177, 115–125.
Suzuki SW, Chuang Y-S, Li M, Seaman MNJ, Emr SD (2019). A bipartite sorting signal ensures specificity of retromer complex in membrane protein recycling. J Cell Biol 218, 2876–2886.
Suzuki SW, Emr SD (2018). Membrane protein recycling from the vacuole/lysosome membrane. J Cell Biol 217, 1623–1632.
Suzuki SW, Oishi A, Nikulin N, Jorgensen JR, Baile MG, Emr SD (2021). A px-bar protein mvp1/snx8 and a dynamin-like gtpase vps1 drive endosomal recycling. Elife 10, e69883.
Takar M, Wu Y, Graham TR (2016). The Essential Neo1 protein from budding yeast plays a role in establishing aminophospholipid asymmetry of the plasma membrane. J Biol Chem 291, 15727–15739.
Tu Y, Seaman MNJ (2021). Navigating the controversies of retromer-mediated endosomal protein sorting. Front Cell Dev Biol 9, 658741.
Valdivia RH, Baggott D, Chuang JS, Schekman RW (2002). The yeast clathrin adaptor protein complex 1 is required for the efficient retention of a subset of late Golgi membrane proteins. Dev Cell 2, 283–294.
Varadi M, Anyango S, Deshpande M, Nair S, Natassia C, Yordanova G, Yuan D, Stroe O, Wood G, Laydon A, *et al.* (2022). AlphaFold protein structure database: Massively expanding the structural coverage of protein-sequence space with high-accuracy models. Nucleic Acids Res 50, D439–D444.
Vilariño-Güell C, Wider C, Ross OA, Dachsel JC, Kachergus JM, Lincoln SJ, Soto-Ortolaza AI, Cobb SA, Wilhoite GJ, Bacon JA, *et al.* (2011). VPS35 mutations in parkinson disease. Am J Hum Genet 89, 162–167.
Voos W, Stevens TH (1998). Retrieval of resident late-Golgi membrane proteins from the prevacuolar compartment of Saccharomyces cerevisiae is dependent on the function of Grd19p. J Cell Biol 140, 577–590.
Wiederkehr A, Avaro S, Prescianotto-Baschong C, Haguenauer-Tsapis R, Riezman H (2000). The F-Box protein Rcy1p is involved in endocytic membrane traffic and recycling out of an early endosome in Saccharomyces cerevisiae. J Cell Biol 149, 397–410.
Wu Y, Takar M, Cuentas-Condori AA, Graham TR (2016). Neo1 and phosphatidylethanolamine contribute to vacuole membrane fusion in Saccharomyces cerevisiae. Cell Logist 6, e1228791.
Xu P, Baldridge RD, Chi RJ, Burd CG, Graham TR (2013). Phosphatidylserine flipping enhances membrane curvature and negative charge required for vesicular transport. J Cell Biol 202, 875–886.
Xu P, Hankins HM, MacDonald C, Erlinger SJ, Frazier MN, Diab NS, Piper RC, Jackson LP, MacGurn JA, Graham TR (2017). COPI mediates recycling of an exocytic SNARE by recognition of a ubiquitin sorting signal. Elife 6, e28342.
Zhou X, Graham TR (2009). Reconstitution of phospholipid translocase activity with purified Drs2p, a type-IV P-type ATPase from budding yeast. Proc Natl Acad Sci USA 106, 16586–16591.
Zimprich A, Benet-Pagès A, Struhal W, Graf E, Eck SH, Offman MN, Haubenberger D, Spielberger S, Schulte EC, Lichtner P, *et al.* (2011). A mutation in VPS35, encoding a subunit of the retromer complex, causes late-onset parkinson disease. Am J Hum Genet 89, 168–175.